

Dalton Transactions

Accepted Manuscript



This is an *Accepted Manuscript*, which has been through the Royal Society of Chemistry peer review process and has been accepted for publication.

Accepted Manuscripts are published online shortly after acceptance, before technical editing, formatting and proof reading. Using this free service, authors can make their results available to the community, in citable form, before we publish the edited article. We will replace this *Accepted Manuscript* with the edited and formatted *Advance Article* as soon as it is available.

You can find more information about *Accepted Manuscripts* in the [Information for Authors](#).

Please note that technical editing may introduce minor changes to the text and/or graphics, which may alter content. The journal's standard [Terms & Conditions](#) and the [Ethical guidelines](#) still apply. In no event shall the Royal Society of Chemistry be held responsible for any errors or omissions in this *Accepted Manuscript* or any consequences arising from the use of any information it contains.

Functionalization of Mesoporous Materials for Lanthanide and Actinide Extraction

Justyna Florek^{a,b,*}, Simon Giret^{a,b}, Estelle Juère^{a,b}, Dominic Larivière^{a,c}, and Freddy Kleitz^{a,b,*}

a) Université Laval, Department of Chemistry, Québec, QC, G1V 0A6, Canada;

Tel: +1-418 656-2131 ext. 7812;

E-mails: freddy.kleitz@chm.ulaval.ca; justyna-agata.florek.1@ulaval.ca

b) Centre de Recherche sur les Matériaux Avancés (CERMA), Université Laval, Québec, QC, G1V 0A6, QC, Canada

c) Centre en Catalyse et Chimie Verte (C3V) Université Laval, Québec, QC, G1V 0A6, Canada

Abstract

Among the energy sources currently available that could address our insatiable appetite for energy and minimize our CO₂ emission; solar, wind, and nuclear energy currently occupy an increasing portion of our energy portfolio. The energy associated with these sources can however only be harnessed after mineral resources containing valuable constituents such as actinides (Ac) and rare earth elements (REEs) are extracted, purified and transformed in components necessary for the conversion of energy into electricity. Unfortunately, the environmental impact resulting from their manufacturing including the generation of undesirable and, sometime, radioactive wastes, and the non-renewable nature of the mineral resources, to name a few, have emerged as challenges that should be addressed by the scientific community. In that perspective, the recent development of functionalized solid materials dedicated to selective elemental separation/pre-concentration could provide answers to several of the above-

mentioned challenges. This review focuses on the recent advances in the field of mesoporous solid-phase (SP) sorbents designed for REEs and Ac liquid-solid extraction. Particular attention will be devoted to silica and carbon sorbents functionalized with commonly known ligands, such as phosphorous or amide-containing functionalities. The extraction performances of these new systems are discussed in terms of sorption capacity and selectivity. In order to support potential industrial applications of the silica and carbon-based sorbents, their main drawbacks and advantages are highlighted and discussed.

Keywords: Lanthanides (Ln); Actinides (Ac); Rare Earth Elements; Solid-Phase Extraction; Mesoporous Sorbents; Metal Purification, Waste Disposal; Pre-concentration; Extraction Chromatography

Introduction

Due to the rapidly growing energy demand, the transition to carbon-free economy, the non-sustainable character of many of our natural resources and the importance of protecting our environment and our health, the selective extraction/recovery of valuable rare earth elements (REEs) and actinides (Ac) from various sources, including mining, industrial and urban wastes, has become an important issue.^{1,2} Additionally, the expansion and modernization of the current infrastructures designed for energy production, such as nuclear power plants and wind turbines, are major ecological, social and security concerns.^{3,4,5} As an example, the demand for REEs has drastically increased over the last thirty years, mostly because of the rapidly growing production of economically important applications such as car catalysts (Ce), hybrid vehicles (Dy, La, Nd) or modern green energy technologies such as wind turbines (Pr, Nd, Sm, Dy), batteries (La) or fluorescent and luminescent phosphor lamps (La, Gd Tb, Eu, Yb).⁶ These needs, combined with the monopolistic policy of the REEs market, recently noted by several government

agencies, such as European Union Commission and US Department of Energy, have raised awareness regarding our current and future needs in REEs. Both organizations consider the REEs as the most critical raw material groups with the highest supply risk.^{7,8} Therefore, it is already noticeable that many countries have intensify their prospection/mining efforts regarding these elements. Furthermore, the majority of available REEs is currently acquired by mining in the natural environment, the commercial recycling of REEs remaining low and insufficient, *i.e.*, only around 3% of the REEs were being recycled in 2011.⁹

Along with our growing need for REEs, the energy demand is likely to increase over the next several decades³, which combined with our global effort to limit the magnitude of climate changes, should inevitably initiate new ventures in energy production based extensively on newer and marginal sources, such as solar, wind, and nuclear energy. Although the latter one has demonstrated over the last 50 years its reliability to produce cost-effective electricity at a constant rate, it is still regarded by many as a risky approach for energy production. Health and environmental concerns associated with uranium mining operations, the main production source of uranium used as fuel in most commercial nuclear power plants, are often expressed by local communities to nuclear regulators or environmental assessment committees. Moreover, the recent radiological event at Fukushima and its repercussions on population, environment and agriculture, highlighted the urgent need for continuous, fast and trace-sensitive monitoring of radioactive releases and newer strategies for the long-term management of legacy wastes and contaminated lands.

While both REEs and Ac can be found naturally in minerals deposits worldwide and are not as rare as their name implies, the true economical value of these elements as vectors for technological applications and energy sources is only reached when they are isolated and thoroughly purified from the mineral matrix and from each other's. As an example, the presence of other REEs as impurities diminishes the efficiency of electronic/optic devices based on a specific lanthanide. This isolation of a particular element can only be achieved by the development of hydrometallurgical processes.

General Aspects

Extraction process: approaches and challenges

The traditional way for the recovery of REEs and Ac from minerals is through hydrometallurgy processes (Figure 1). In general, in the first step, the minerals or ores are exposed to acidic (*e.g.*, HF, H₂SO₄) or basic (*e.g.*, NaOH) leaching conditions. However, the leaching step is often non-selective and beside the targeted elements, large amounts of competing elements are also dissolved, thus demanding additional purification steps prior to elemental separation. Uranium, for instance, is leached in strong acidic conditions (*i.e.*, H₂SO₄) from grinded ores. The sulfato-complex formed with hexavalent uranium is subsequently pre-concentrated using liquid-liquid extraction (LLE) with quaternary amines in kerosene which eliminates the majority of the undesired mineral species, before being subjected to ammonia neutralization and temperature treatments to produce U₃O₈ (yellow cake). Further treatments, using tri-*n*-butyl phosphate (TBP), for example, have to be performed to achieve the significant level of purity required for nuclear fuel production.¹⁰ Such treatment, based on selective lanthanide or actinide separation is, however, far more challenging. In case of the REE separation, the first purification step includes only a preliminary separation of metals into broad groups, *i.e.*, light rare earth elements (LREEs; La-Nd), SEG (*i.e.*, Sm, Eu, Gd) and heavy rare earth elements (HREEs; Tb-Lu, Y). Unfortunately, a specific element often cannot be separated from the elements composing these groups in a simple and economic way due to their very similar physicochemical properties.¹¹ In addition, the uneven distribution of individual Ac and REEs composing common ores/minerals or spent fuel^{12,13} further complicate the separative process.

Industrially, various methods including extraction, adsorption, ion-exchange or chemical precipitation, can be used to recover rare earth metals or actinides from aqueous solutions. Owing to its good selectivity and significant separative performances, liquid-liquid extraction (LLE, Figure 2) is

considered as a method of choice for such task.¹⁴ However, in order to obtain high purity fractions of REEs or Ac required for industrial applications, multiple sequential extraction steps are usually required, that can be carried out either in continuous or batch system. The number of separation steps increases with the requirement in purity of each element produced. Pure REE oxides are generally obtained after LLE via calcination of oxalate salts obtained after precipitation of the dissolved REEs in the concentrated solution. Finally, pure metallic forms can be prepared either by molten salt electrolysis or metallothermic reduction.¹⁵

Industrial extractants used in LLE of REEs or Ac contain mostly oxygen, nitrogen, sulfur and/or phosphorous atoms. Among the different ligands reported in the literature, a large portion are carboxylic-based ligands (such as ethylenediaminetetraacetic acid, EDTA, and its derivatives), sulfoxide derivatives (RR'SO), quaternary ammonium salts (usually in the presence of chelating agents like EDTA, diethylenetriaminepentaacetic acid, DTPA), amines, amides (diglycolamide-type ligands, DGA or malonamide, MA), organophosphoric analogues, such as 2-ethylhexyl phosphoric acid (HDEHP), TBP and calixarenes, pillararenes or tripodal framework-based ligands (Figure 3).¹⁶ The choice of the extracting medium depends not only on the extraction affinity of the ligand, its separation factors and its solubility, but also on the economic costs. Unfortunately, the amount and the nature of the wastes generated following the multiple sequential extractions necessary for the industrial preparation of the pure or oxidized forms of REEs and Ac from mineral ores or spent fuels do not fit many of the green chemistry and engineering principles^{17,18} and overshadow the greener and cleaner potential of the technologies relying on these elements. Moreover, many of the extractants used in LLE extraction (*i.e.*, cationic, anionic or neutral exchangers) suffer from either slow extraction kinetics, low solubility in aliphatic diluents, degraded performances in acidic conditions or lack of reusability,^{19,20,21} rendering the LLE procedures, although being relatively straightforward, solvent- and time-consuming while producing large amount of environmentally toxic/harmful wastes.²² In addition, in many LLE systems, the formation of a three-phase

system (emulsions) can be observed and needs to be addressed.²³ A number of research groups have proposed the use of ionic liquids (ILs) as an alternative to more conventional solvents used in LLE. This interest in ILs as a greener option for LLE is driven by the fact that they have unique properties such as negligible vapor pressure, good thermal stability, miscibility in water or organic solvents and good extraction capacities.²⁴ While being an interesting avenue, researchers in the field of ILs still need to address the issues of low solubility of numerous extractants in them, especially phosphorous-based ligands, and the difficulty related to back-extraction of the metal species due to the strong interactions between ILs and the targeted metals,^{25,26} before this approach can reach its full potential.

The greener nature of the extraction/pre-concentration procedure can also be explored from the liquid-solid extraction perspective, *i.e.*, solid-phase extraction (SPE) or solid-liquid extraction (SLE) methods, where one of the liquid phases is reduced/eliminated. In industry, the most common supports used for the separation/purification steps are ion-exchange (IEC) and extraction (EXC) chromatographic-based resins.²⁷ Typically, the backbone of most of the resins consists of an insoluble polymer matrix and the most classical ones are based on cross-linked polystyrene. A variety of functional groups can be introduced either by co-condensation of functional monomers or by physical mixture of different polymers. Most of the sorbents used for the extraction/separation steps are based on the “physical” addition (impregnation) of the ligands to the solid support which in turns often results in leaching problems, limiting the lifetime of the resins.^{27,28} Moreover, as a result of stripping of the extractant, diminishing extraction performances are often observed.²⁸ In contrast, IEC resins offer good separation capacity and reusability, but lack of the elemental selectivity required for the ultra-trace separation. To overcome these limitations, the development of the new extraction strategies, such as SPE has emerged over the past few years.^{29,30} Especially, the SPE approach usually provides shorter extraction times, greater separation factors and better reusability than its LLE counterpart. These inherent benefits could eventually translate into reduction of costs and environmental footprints.

Therefore, we need to support research strategies targeted towards the development of environmentally friendly and cost-effective purification sorbents aimed at better extracting/separating of REEs and Ac. In this context, it may be expected that mesoporous materials,^{31,32,33} which show very attractive properties as solid-phase chromatographic supports, could become a support of choice for such type of separation. First, these materials exhibit remarkably high specific surface area (S_{BET}) allowing for high contact efficiency, and thus, enhancing adsorption capacity while reducing extraction time. In addition, because of the chemical anchoring of the ligand on the pore surface through covalent bonds, the thus-synthesized porous sorbents should exhibit greater regenerative capacities, ultimately increasing their marketable potential. Furthermore, these functionalized solid sorbents owing to their selective and effective extractive natures should enable the purification of REEs and Ac with a limited number of separation steps, which should translate positively in term of waste reduction.

Requirements for SPE sorbents and benefits of mesoporous materials

Depending on the type of extracted elements, extraction conditions or application, a well-designed solid sorbent should have the required particle size, shape, morphology and selective ligands properly attached. In addition, in case of the dynamic high pressure separation systems, the solid sorbent should be characterized by a well-developed pore structure with tunable pore size, pore connectivity and surface properties. Finally, the possibility of regeneration of the sorbent in cost-effective and environmentally friendly manner is a key attribute. Traditionally, bare silica gels, chemically modified (bonded) silica and activated carbon materials are the most common sorbents used as solid-phase separation supports.^{34,35} More recently, several other materials have been successfully applied for metal sequestration, such as nanoporous (ordered) silica^{36,37,38} and carbon materials³⁹, metal oxides (titanium or iron),^{40,41} *self-assembled monolayers on mesoporous supports* (SAMMS),^{16,42} silica microspheres^{43,44} or silica monoliths,⁴⁵ to name a few only. In addition, a lot of interests have also been devoted to metal-organic-framework

(MOF) materials as efficient chromatographic solid-phases.^{46,47} Such interest in the MOF materials is the result of their high and easy tunable porosity, which can be modulated by simply varying the length of the organic bridges (linkers) in their hybrid structure. Furthermore, additional organic ligands can be introduced in these structures via pre-installation, coassembly and post-functionalization methods.⁴⁸ However, despite the growing interest for MOFs as stationary phases, their commercial and industrial applications remain hampered by several challenging issues, such as prohibitive production cost or inadequate stability in the extraction conditions, for instance.

In general, the undoubted advantage of porous supports is their particularly high surface area that allows for a high degree of functionalization, which in turns leads to the increased extraction capacity of these materials, in comparison with nonporous sorbents.⁴⁹ Ordered mesoporous solids, such as MCM-41 and SBA-15-type silicas^{50,51,52} exhibiting pores comprised between 2-30 nm, are attractive as selective sorbents and supports, and suitable as stationary phases in chromatographic applications.^{53,54,55} These robust silica materials contain pores in the nanometer range (by definition, mesopores are between 2 and 50 nm⁵⁶) and can easily be prepared through a combination of templating methods using micellar aggregates and inorganic sol-gel processes, generally in aqueous conditions.^{57,58,59} The use of micelles of amphiphilic molecules or block copolymers, which serve as structure-directing agents (SDAs), enables specific formation of pores with well-defined size and shape. The thus-templated ordered mesoporous silicas demonstrate exceptional long-range ordering, narrow pore size distribution, high surface area ($S_{\text{BET}} > 1000 \text{ m}^2 \text{ g}^{-1}$) and high pore volume ($> 1.0 \text{ cm}^3 \text{ g}^{-1}$). These materials are considered as non-toxic, chemically and thermally stable. Furthermore, surface silanol groups (Si-OH) allow fixation of a great diversity of functionalities through coupling reactions with organosilanes.^{60,61,62,63,64} Such modified mesoporous silica supports have previously been studied for selective capture and removal of heavy metal cations and radio-pollutants.^{49,65,66,67}

In particular, large pore ordered mesoporous silicas, such as SBA-15^{68,69} and KIT-6⁵² (Figure 4),⁷⁰

represent an excellent starting point for the design of new extraction agents for separation of REEs and Ac. These mesoporous silica materials are easily synthesized in acidic media in the presence of polyethylene oxide-co-polypropylene oxide triblock copolymers (*e.g.*, Pluronic P123, BASF) in combination to a silica precursor (*e.g.*, tetraethylorthosilicate, TEOS).⁷¹ The resulting silica powders possess high surface area ($\geq 800\text{-}1000\text{ m}^2\text{ g}^{-1}$, suitable to place a large number of ligands), high pore volume ($> 1\text{ cm}^3\text{ g}^{-1}$) and large pores (6-13 nm), advantageous for heterogeneous separation process involving a liquid phase. Also, tailoring of pore size, pore shape and pore connectivity of these templated silicas is possible to optimize adsorption and diffusion parameters of substances in solution.^{31,72,73} Morphology and dimension of the particles can be controlled and the materials can be processed into monolithic objects.⁷⁴ Mesoporous SBA-15 silicas and related materials are therefore ideal candidates to act as supports for locating large amounts of highly accessible functional species serving as ion-exchangers and/or extraction entities. In addition, their framework structure and pore topology should allow for possible control of the spatial arrangement of functional groups. Functionalities such as organic ligands and functional polymers may be located selectively on the mesopore surface, encapsulated inside the channels, or even inside the inorganic framework walls. For instance, silica modification can be done in a one-pot approach, either by the immediate reaction of tetraalkoxysilanes and terminal trialkoxyorganosilanes (*i.e.*, co-condensation) in the presence of the structure-directing agents, or by the use of bridged di-silane precursors which yield periodic mesoporous organosilicas (PMOs).⁶⁴ In these latter cases, the organic groups are apparently more evenly distributed on and in the silica walls, possibly limiting pore blocking problems. However, high amount of the silylated organic compounds in the synthesis media often leads to materials with rather low mesostructure quality.

In case of such silica-based materials, abundance of the silanol groups allows for the efficient and easy functionalization through condensation reactions producing siloxane species (*e.g.*, grafting procedure), which are quite stable in the pH range commonly used for REE or Ac extraction, *i.e.*, pH 3 to 8.⁷⁵ The

concentration/density of the silanol groups affects the amount of grafted organic species and consequently sorption capacity, selectivity and hydrophilic/hydrophobic character of the sorbent.⁷⁶ Conveniently, the amount and concentration of surface silanols, before or after surface functionalization, may be controlled by different methods, including acid treatment for re-hydroxylation,^{77,78} hydrothermal treatment,⁷⁹ and passivation with trimethylsilyl groups (*e.g.*, trimethylchlorosilane, hexamethyldisilazane).⁸⁰ Regarding a possible role of these silanols on extraction, the extraction behavior of non-functionalized silica (*e.g.*, SBA-15 or MSU-H) was verified by Lin et al.⁸¹ and Guo et al.⁸² who suggested high uranium physisorption by bare silicas. Moreover, the results indicate that the un-modified silica material has relatively fast adsorption kinetics (< 30 min) with a high maximum adsorption capacity. Thus, since residual silanols may be present in grafted materials, the influence of these groups should not be always neglected when studying (functionalized) mesoporous supports for extraction chromatography applications.

However, since siliceous-based compositions (SiO₂ frameworks and Si-C linkages) might present issues with their chemical stability under some of the operating/treatment conditions (strong acidic medium), other supports are also envisioned on the basis of carbon-based frameworks. Nanoporous carbon equivalents of mesoporous silica are expected to better tolerate harsh acidic or basic conditions. Ordered mesoporous carbons,^{83,84,85} with proper pore-surface functionalization, are thus also suggested as high surface area supports for immobilizing extraction agents. The synthesis of highly ordered mesoporous carbons is known since 1999 on the basis of the hard templating method (*i.e.*, *nanocasting*), yielding materials with exceedingly high surface area and well-structured pore network (*e.g.*, CMK-type frameworks).^{86,87,88} In the case of the nanocasting method, porous silica usually serves as a mold and a selected carbon precursor, such as sucrose or furfuryl alcohol, is impregnated inside the pores, polymerized and carbonized. Finally, the silica template is dissolved and removed using basic (NaOH) or acidic (HF) conditions (Figure 5). However, these protocols using porous silica as solid templates are

tedious and rather difficult to apply at a larger scale. Since 2005, it is possible to assemble carbon mesophases from the combination of phenolic-type resins⁸⁹ and triblock copolymer templates through a cooperative self-assembly,^{83,90,91} in a similar way as for the silica analogues. These resins are then treated thermally and converted into highly porous mesostructured carbons, under controlled atmosphere (without the need of silica template) (Figure 5).⁸³ The resulting carbon structures are chemically and thermally stable and it is possible to adjust their porosity features quite well. Carbon powders exhibiting specific surface area (S_{BET}) over $1600 \text{ m}^2 \text{ g}^{-1}$ with pore sizes $\sim 6 \text{ nm}$, and different pore structures including 2D hexagonal and 3D cubic (also analogues of the 3D cubic KIT-6 silica) can be synthesized by this method. The texture properties and morphology can be controlled by varying synthesis conditions (pH, time, and temperature), gel compositions, use of organic additives, and type of copolymer structure-directing agents.^{85,92} For such compositions, one could expect greater chemical, thermal and radiation stabilities, which are usually not altered through the surface functionalization of carbons.^{93,94,95}

Permeability and stability issues

It has been well-documented that in case of dynamic (column) separation systems the decrease in particle size results in significant enhancement of efficiency and shorter analysis time. Indeed, the chromatographic resolution is inversely proportional to the square root of the particle size, *i.e.*, when the particle size decreases, an improvement in terms of peak efficiencies and resolution is observed.⁹⁶ Consequently, converting the stationary phase of chromatographic columns from the microscopic to nanometric scale can significantly improve peak efficiencies and resolution. Nevertheless, this relationship between chromatographic performances and stationary phase scale has its practical limitation as it is difficult to build well-packed chromatographic columns with small particles and that the quality of the packing will greatly influence the mobile phase permeability, ultimately resulting in back-pressure issues. Thus, ordered mesoporous materials with well-developed porous structure and properly tethered

chelating ligands might provide a solution to such solvent transport in the packed-bed column systems, and therefore, they could overcome transportation/pressure concerns. Within this context, the reported bimodal mesoporous-macroporous silica monoliths⁷⁴ seem to be the most promising materials. In this case, the macroporous pores (pore size > 50 nm) allow the mobile phase to easily permeate through the support, while smaller voids provide the surface area for insertion of a stationary phase. As depicted in Figure 6, organic monoliths and silica monoliths can substantially lower the back pressure, in comparison with silica particles-based columns.^{97,98} Based on this bimodal design, macropores in monolithic systems should provide easier access to the active sites (*e.g.*, sorption sites) resulting in enhanced chromatographic performances.⁹⁹ The first porous monolithic silica materials were prepared in 1991 by the Nakanishi group, in the presence of poly-(sodium styrene sulfonate), based on a sol-gel process.¹⁰⁰ Later, mesoporous-macroporous silica monoliths were synthesized by using a variety of templates, such as block co-polymers (*e.g.*, Pluronic P123, Pluronic F127)^{101,102} and cationic or anionic surfactants,^{103,104} in a similar sol-gel process in the presence of polyethylene oxide and a silicon source (*e.g.*, TEOS). There are several benefits associated with such silica monolithic supports, which make them interesting candidates as stationary phases in dynamic separation systems: desirable mass transfer properties, as discussed previously, but also the possibility to impose specific permanent shapes or morphologies to the support during the synthesis and the facility of pore surface functionalization. Monoliths have been prepared in a variety of morphologies or shapes, including columns, disks or capillaries.^{103,105} Typically, the shape of the silica-based monoliths is dictated and modulated according to the shape of the flask (mold) involved in the synthesis. In addition, by varying surfactant species and processing conditions, *i.e.*, by carefully controlling the phase separation and gelation processes, diverse mesoporosities can be induced. This versatility in shapes and morphologies is particularly interesting when transitioning monolithic structures into current industrial applications. The use of silica as building blocks for monolithic structures allows to use relatively simple synthetic protocols for the tethering of different silane-based ligands on the surface,

^{90,98,106} opening up a world of new opportunities in term of selectivity and applications. The surface modification can be done in a similar manner as for silica powders, either by post-synthesis modification (grafting) or by wet impregnation (physisorption).

Regrettably, an important limitation of the silica-based materials arises from their limited stability in strongly acidic/basic conditions. This issue is particularly important because, typical Ac/REE separations are performed in harsh chemical conditions. Commonly, silica-based materials are mostly stable in pH conditions ranging from 3 to 8.^{68,107,108} Beyond this pH range, the silica support becomes more brittle (pH > 8) or its surface functionalization can be altered as the results of Si-C bond cleavage (pH < 3). The applicable pH range can be enlarged by replacing the silica supports by a carbon-based matrix, such as activated carbon. However, the main limitation of activated carbons is the abundance of micropores (*i.e.*, pore size < 2 nm) which significantly limit diffusion inside the pores. Hence, a great deal of attention has been recently given on other types of carbons, namely carbon nanotubes, aerogels and the ordered mesoporous carbons described above. Until now, two types of the mesoporous carbon materials were tested for extraction applications: 1) hard templated carbons^{87,88} and 2) soft templated carbons.^{90,91} In both cases, surface modification needs to be performed to anchor the selected chelating ligands for REE and Ac extraction applications. This is usually performed in a two-step sequence, *i.e.*, a first oxidation step followed by the proper ligand anchoring.^{109,110} Although current pathways used to obtain functional carbon materials show many similarities with the approaches applied for silica synthesis, an easy and efficient post-synthesis carbon surface functionalization, equivalent to the silica modification, is still missing. Alternatively, there is growing interest for biomass-derived carbons (so-called “hydrothermal carbons”, HTC^{111,112}), which could provide a sustainable source for high surface area sorbent materials. These carbon materials (HTC) present some interesting advantages: 1) an abundance of oxygen functional groups on the surface, which should facilitate the subsequent functionalization; 2) the common HTC carbon sources are inexpensive and widely available (*e.g.*, from cellulose, sugars, other biomass sources);

and 3) the inherent characteristics of carbon materials, such as greater chemical, thermal and radiation stability, are usually not altered by the surface functionalization.

Finally, another important concern that should be taken into account during the development of new solid-phase sorbents for actinides separation is their radiation stability. It is a critical issue as these sorbents will be exposed to significant levels of irradiation based on the chromatographic separation they are intended to perform. For example, sorbents used for spent fuel reprocessing could be exposed to over 400 Gy h⁻¹ in addition to significant heat resulting from the nuclear decays occurring within the pellets.¹¹³ The long term resistance to radiolysis is also beneficial and highly desired in case of automated, on-line detection systems, especially when performed on active components of a nuclear power plant.

Solid-phase sorbents used for Actinide sorption

In the recent years, considerable attention has been directed towards the development of new solid-phase extraction methods and materials for entrapment of environmentally toxic and radioactive elements, in light of the Fukushima-Daiichi event, and also on uranium decontamination and enrichment.^{16,36,114,115} Uranium ions are mostly extracted during the acid mine drainage or during the nuclear fuel production from natural sources. Traditionally, the most common method used for Ac separation is liquid-liquid extraction, where various organic extracting agents, such as phosphorous-based ligands, amines or sulfoxides, are employed (see Figure 3).¹¹⁶ Among them, organophosphate-based ligands are known to have high extraction capacity, affinity and selectivity towards ions such as uranium ions. Later, the same chelating ligands have been chemically attached to solid-phase supports, like polymeric resins or silica and carbon materials.^{16,36,114} A compilation of most common ligands and supports used for Ac solid-phase separation is given in Table 1.

Phosphorous-containing ligands

One of the most important ligand families with high affinity towards actinides are the organic molecules containing phosphorous-based functionalities such as phosphates, phosphonates or organophosphorous derivatives. Among this category of ligands, tributyl phosphate (TBP) and carbamoylmethylphosphine oxide (CMPO) have found commercial applications in so-called Plutonium Uranium Redox EXtraction (PUREX) and TRansUranic EXtraction (TRUEX) in aqueous nuclear reprocessing method for the recovery of actinides.^{117,118}

Although the UO_2^{2+} extraction complexes with CMPO ligand have been explored in the literature, many unanswered questions still remain, for example, the structures of the corresponding complexes.^{119,120,121} For instance, it has been proposed that uranyl- NO_x complex with CMPO is formed from two bidentate nitrate groups and one bidentate CMPO unit is spread around the equatorial plane of uranyl. On the other hand, hexagonal bipyramidal complex, $\text{UO}_2(\text{NO}_3)_2(\text{CMPO})_2$, was suggested by Horwitz et al.¹²² More recently, Shi et al.¹²³ investigated the equilibrium geometries and stabilities of the UO_2^{2+} extraction complexes with CMPO ligand. It was found that the 1:1-type complexes are coordinated as bidentate chelating ligands through the carbonyl oxygen and phosphoryl oxygen atoms. However, for the 2:1-type complexes CMPO mainly coordinates U ions by the phosphoryl oxygen atom. Moreover, it has been indicated that metal-ligand bonding is mainly ionic, and the phosphoryl oxygen atoms of CMPO have stronger coordinating ability to the metal cations than the carbonyl oxygen atoms.

Owing to the complexing abilities of phosphorous-containing ligands, it is not surprising that they were selected by many research groups, including ours, as potential tethering groups for actinide separation on mesoporous support. Functionalized silica-based solid supports with phosphorous-containing ligands exhibited decent extraction performances. At the moment, our team has used large-pore mesoporous silica materials, such as SBA-15, SBA-16 and KIT-6 materials, functionalized with 2-diethylphosphatoethyl-triethoxysilane (DPTS) for the sorption of uranium in various extraction

conditions.^{36,114} These studies also highlighted the importance of the solid support, its morphology, pore connectivity and pore shape, on the extraction behavior of DPTS-functionalized materials. It appeared that DPTS-functionalized large pore 3D cubic KIT-6 material, which exhibits highly interconnected pore structure with narrow pore size distribution, possesses excellent extraction properties towards U(VI); *i.e.*, 40 times higher than the commercially available U/TEVA (EXC) resin. Moreover, this sorbent was found to be superior to its 2D structural equivalent, *e.g.*, SBA-15 material (Table 2). It was postulated that the 3D connectivity of the KIT-6 support provides a better accessibility to the surface, both during the grafting and the extraction stages, thus enhancing extraction properties.³⁶ Furthermore, results from the dynamic extraction system revealed an excellent stability and reusability of this system. For example, even after several extraction/elution cycles, the material maintained its structural and chemical nature with unchanged sorption capacity. Also, this mesoporous sorbent displayed fast adsorption kinetics with equilibrium states reached within 1 min, a factor of ten faster than commercial resin (U/TEVA).¹²⁴ The uptake of uranium ions by the KIT-6-based sorbent seemed facilitated because of the presence of the large pores (pore size > 6 nm) which are more advantageous when dealing with adsorption from liquids, together with a well-preserved high surface area. A similar influence of the dimensionality of the mesostructure of the support (*e.g.*, 2D vs. 3D) on the extraction capacity had been discussed already in 2001 by Vidya et al.¹²⁵ or more recently by Juère et al.¹²⁶ In another example, spherical mesoporous silica nanoparticles (ca. 100 nm) functionalized with DPTS by the one-pot co-condensation of DPTS and tetraethoxysilane (TEOS), were synthesized by Shi and co-workers.¹²⁷ These materials exhibited maximum uranium capacity above 300 mg g⁻¹ and short equilibrium time – typically below 30 min. Again, the functionalized silica sorbent did not show evidence of decrease in the sorption capacity during the reusability studies.

Other kinds of phosphorous-containing derivatives, such as ethylphosphonic acid or phosphine oxides, were also suggested and used as the chelating agents for Ac extraction, with more or less success. For

instance, Chen et al.⁸⁰ functionalized SBA-15 silica by post-grafting method using phosphonate derivatives: diethylethylphosphonate (DEP) and ethylphosphonic acid (PA), and discussed the influence of different functional groups on the U(VI) uptake. Interestingly, the SBA-15-DEP material exhibited lower sorption capacity than pure SBA-15, which according to the authors was caused by the pore blocking from the grafting procedure and unfavorable configuration of the functional groups (the steric hindrance) on the surface of the SBA-15-DEP sorbent. On the other hand, the SBA-15-PA material displayed an enhanced maximum capacity with required selectivity for U(VI) over a range of competing elements and good reusability properties. Clearly, these observations highlight the critical role of performing adequate pore surface functionalization (*e.g.*, ligand grafting) without pore obstruction. Trialkylphosphine oxide ligands are another interesting class of chelates that are commercially used for Ac (or REEs) sorption, mostly because of their high stability in radioactive and acidic conditions. Thereby, organophosphorous-functionalized mesoporous silica sorbents containing alkylphosphine oxide ligands with variable aliphatic chain lengths were tested for the extraction of U ions from acidic solutions.¹²⁸ Unfortunately, these modified materials showed only moderate sorption capacity, *i.e.*, between 30-40 mg g⁻¹ in pH 4.5. Better extraction capacities were observed at higher pH (pH 6) being about 80-100 mg g⁻¹.

In another study, Lin and co-workers⁹⁵ investigated the influence of different functional groups, such as amidoxime, phosphoryl, and carboxyl groups, grafted on mesoporous carbon on the uranium adsorption capacity in acidic (pH 4) and simulated sea water conditions (pH 8.2). Among the various materials studied, a phosphoric acid-derived sorbent showed the highest sorption capacity in both extraction conditions, *i.e.*, acidic water (97 mg g⁻¹) and artificial seawater (67 mg g⁻¹), despite having the lowest ligand loading. Moreover, kinetic studies revealed rapid and sharp U(VI) sorption in the simulated seawater conditions, *i.e.*, the equilibrium was reached below 3 min. In case of the acidic water sample (pH 4), the uranium uptake was more gradual and clearly two steps could be distinguished, *i.e.*, in the first

step the majority of uranium ions (around 80%) are adsorbed below 5 min and the second step leads to equilibrium in about 30 min.

While most of the efforts in the field of phosphorous-based ligands grafted on solid supports for Ac extraction have been oriented towards uranium, Fryxell et al. investigated the uptake of Th(IV) from aqueous solution by materials designated as SAMMS containing amino or/and phosphonate groups.¹²⁹ MCM-41 silica modified with a monolayer of glyciny-urea functionalities revealed a greater affinity for Th(IV) than for other competitive elements present in the extraction solution, such as Am(III), Pu(IV), Np(V) and U(VI). In this area, our group also investigated simultaneous Th(IV) and U(VI) extraction using phosphonate groups (DPTS-modified mesoporous silica materials).¹¹⁴ In case of the single metal extraction solution, the level of Th(IV) extraction was very high, around 94 %. The experiments performed in the presence of other elements, *i.e.*, U, showed only slight decrease in the Th(IV) capacity, being about 92 %.

Nitrogen-containing ligands

Another common ligand family for actinide extraction is based on nitrogen-containing extractants. One of such extractant groups are the amino-containing compounds, which exhibit interesting extraction behaviors resulting from the amphoteric amidoxime moieties ($-\text{C}(\text{NH}_2)=\text{N}-\text{OH}$), although the binding mechanism between ligand molecules and hexavalent uranium ions is still unclear. In general, the lone pairs of electrons in amino nitrogen and oxime oxygen can donate electrons to the positive metal center and form a stable complex with U(VI). Rao et al.¹³⁰ postulated that oxime oxygen and imino nitrogen are involved in the chelate interactions with metal ions and the bidentate coordination mode is stabilized by the formation of a hydrogen bond between the carbonyl group of glutarimidoxime and water molecule in the hydration sphere of UO_2^{2+} .¹³⁰ Binding between uranyl ion and amidoxime chelating ligands can also occur through amidoxime/amidoximate oxygen atoms or oxygen and nitrogen atoms of the amidoximate anion.^{131,132} Other studies showed that amidoxime group can be deprotonated to form an amidoximate

anion which can further coordinate metal ions.¹³³ However, no experimental proof of the tautomerization of amidoxime group has been provided. Based on the X-ray diffraction analysis (XRD) and density functional theory (DFT) modeling, Hay et al.¹³⁴ investigated several possible chelating interactions, *i.e.*, bidentate chelation of oxygen and amide nitrogen atoms, monodentate binding of either oxygen or nitrogen atoms and η^2 binding with N–O group, where the last form is the most stable one (Figure 7).^{99,135} Further, it has been proposed that formation of the complex is driven by the changes in pH. For instance, at low pH, the hydroxyl groups of oxime and imino groups of amidoxime are protonated, resulting in inferior sorption capacity because of the weaker oxime nucleophilicity. Oppositely, at higher pH the protonation level is lower which favors the complex formation between negatively charged oxygen and uranium atoms. The uncertain binding mechanism of amidoxime-uranium complexes is largely due to the broad range of different pK_a values reported in the literature. Very recently this problem was discussed by Mehio et al.^{136,137} who indicated that pK_a of amidoxime monomer is 5.78, while acyclic amidoxime unit shows higher pK_a value being 6.1.

As a first example of immobilization, polyamidoxime ligands were grafted on micro-mesoporous (organic) copolymer monoliths.⁹⁹ These mesoporous polymers formed of vinylbenzyl chloride (VBC) monomers and divinylbenzene (DVB) cross-linking agent, were tested in synthetic seawater samples and displayed higher uranyl adsorption capacity ($64\text{--}80\text{ mg g}^{-1}$) than commercial sorbents, *e.g.*, alumina-based Dyna-Aqua[®] (21 mg g^{-1}) and titania-based Metsorb[®] (between $12\text{--}46\text{ mg g}^{-1}$) materials.⁹⁹ Moreover, extraction experiments performed on actual seawater aliquots revealed an initial uranium adsorption representing roughly 90 % of the capacity, which was reached in the first 10 days. Subsequently, a slower uptake was observed with no plateau (17 days), suggesting that no equilibrium was reached after 27 days.

Additionally polyamidoxime ligands were also grafted on mesoporous silica powders,^{81,135} polyacrylonitrile-block-polystyrene nanoparticles¹³⁸, silica microspheres,⁴³ mesoporous carbon^{94,109,139} and nanofibrous sorbents.¹⁴⁰ For example, Lin and co-workers⁸¹ used the commercial large-pore 2D MSU-

H silica material modified with several ligands, including the amidoxime-functional groups, for uranium extraction from synthetic seawater aliquots. Interestingly, the amidoxime-functionalized sorbent displayed average adsorption capacity, being around 40 mg g^{-1} and moderate equilibration time – 40 min. According to the authors, the differences in the sorption capacity between amidoxime- and phosphorous-containing sorbents should be attributed to the diverse affinities of the organic moieties for U, rather than to the physical properties of the support (*e.g.*, the porosity features). Likewise, irrespective of the ligand grafted on the silica surface, when water was replaced by simulated seawater the sorption capacity dropped by fourfold.

Jaroniec et al.¹³⁵ synthesized porous amidoxime-functionalized organosilica with ordered mesoporosity and high specific surface area which leads to materials with large number of easily available binding sites. Consequently, the obtained sorbents exhibited high extraction capacity with synthetic seawater samples, being 57 mg U g^{-1} . Unfortunately, the authors did not perform experiments using real seawater aliquots or shown adsorption isotherms and kinetic studies, making the real potential of these sorbents difficult to ascertain. Recently, an interesting sorbent design consisting of magnetic mesoporous microspheres with an inner magnetic core (Fe_3O_4), a middle layer of nonporous silica and an outer layer of amidoxime-functionalized mesopores demonstrated quite high uranium sorption, about 277 mg g^{-1} , and fast equilibration time.⁴⁰ According to the authors, short equilibrium time was provided by the well-defined mesoporous structure of the sorbent, beneficial for the sorption process, and strong metal-amidoxime interactions. In addition, introducing of the magnetic core to the silica host seems to provide an easy and efficient way to quickly remove, separate and further regenerate the magnetic particles, which is of interest for commercial applications. Moreover, both the regeneration and sorption studies (in the presence of competing elements) confirmed the good extraction performance of these materials. Finally, the dissolution of iron during the extraction/regeneration cycles was kept at a low level owing to the silica coating around the magnetic core in the microspheres.

Differently, amidoxime ligands were also bonded to porous carbon nanostructures, *i.e.*, multi-walled carbon nanotubes, in a two-steps procedure. The ligand was formed through grafting of acrylonitrile moieties, followed by the reaction of the cyano groups with neutralized hydroxylamine hydrochloride.¹⁴¹ These modified multi-walled carbon nanotubes (MWCNTs) showed high extraction capacity (145 mg g^{-1} , in the extraction condition tested (pH 4.5) regardless of low surface area of the final material ($S_{\text{BET}} = 72 \text{ m}^2 \text{ g}^{-1}$). This sorption capacity is 10 times higher than the one measured for un-functionalized MWCNTs and 4 times higher than for the oxidized version of this support. In addition, modification with amidoxime significantly increased the selectivity towards uranium ions. It was shown that in the presence of other competing ions, such as Mn, Co, Ba or Fe and V (present as part of simulated seawater conditions), the selectivity towards uranium was preserved for the modified carbon nanotubes. On the other hand, the oxidized material showed, as expected, similar uptake for all the elements and low overall extraction capacity. In another example, good extraction performances using amidoxime ligands were also reported for modified hydrothermal carbon-based nanoparticles, although the synthesized materials possessed negligible amount of mesopores, very low specific surface area ($< 10 \text{ m}^2 \text{ g}^{-1}$) and pore volume ($0.01 \text{ cm}^3 \text{ g}^{-1}$).¹⁰⁹ As suggested by the authors, the presence of a large proportion of oxygen-containing functional groups on the HTC surface, despite increasing the overall sorption capacity, often does not provide higher grafting yield. Consequently, un-functionalized oxygen groups, *i.e.*, carbonyl- or hydroxyl species, could lead to un-targeted metal-ligand interactions which translate into lower sorbent selectivity. Bearing this in mind, Li et al.¹⁰⁹ used glyoxal as a carbon source and minimized the amount of undesired functional groups, which resulted in a material with significantly improved selectivity. Although these amidoxime-functionalized carbon nanoparticles displayed an extremely high U(VI) sorption capacity for mono-elemental batch extraction studies, above 1000 mg g^{-1} , sorption capacity was significantly diminished (approximately 5 times) in the presence of competitive elements at pH 2.5. Moreover, it was observed that the level of uranium uptake was greatly reduced after irradiation of this material; this trend being

accentuated at higher radiation doses. Nonetheless, it was found that the uranium selectivity was mostly unaffected upon irradiation.¹⁰⁹

Immobilized systems for other actinides

SAMMS materials modified with different functional groups such as strong cationic sulfonic acid exchangers, iminodiacetic acid and 3,4-hydroxypyridinone (HOPO), have also been tested for thorium and neptunium extraction.¹⁶ It was shown that the HOPO-SAMMS sorbent exhibited better extraction uptake of thorium than a commercial MnO₂ material and the K_d values reported for this material showed only negligible influence of the nature of the water sample tested (*e.g.*, organic content, salinity, pH, etc.). However, the small particle-based MnO₂ sorbent showed also very good K_d values and the best recovery (log K_d = 4.7–6.2), while only modest recovery was observed for the EDTA-SAMMS and EDTA-based polymeric resin (Chelex 100).¹⁶

Recently, an interesting comparison of plutonium (VI) uptake capacities in batch extraction mode by nanocast ordered mesoporous carbons (CMK-type material) and commercial amorphous activated carbon was performed by the Nitsche group.⁹³ Prior to the extraction experiment, the CMK material was oxidized in nitric acid solution. In contrast to the disordered activated carbon, the oxidized CMK material showed an ordered cubic mesostructure, and higher amount and higher density of oxygen-containing functional groups. The experiments performed showed that oxidized and non-treated CMK carbon materials have greater Pu sorption in pH ≥ 3 than the commercial material, *i.e.*, 58 versus 12 mg g⁻¹, respectively. Moreover, the oxidized CMK sorbent displayed also high Pu capacity in pH 2. The activated carbon sample showed lower Pu uptake in all pH regions tested and interestingly, also slower adsorption rate than the CMK-type sorbents. Furthermore, experiments performed with constant pH (4) but varied Pu concentrations indicated that the oxidized CMK sample has faster Pu uptake from low-concentration solutions and increasing the Pu concentration reduces differences between oxidized and untreated CMK

sorbents. The reusability of CMK sorbents was also tested and it was shown that in pH 4, after addition of concentrated HClO_4 , a complete desorption of Pu occurred generally within 24 h, except for the highest Pu concentration where longer desorption time was needed.

Trivalent actinides are a major part of the radioactive species found in nuclear spent fuel, which are generated in reprocessing plants, thus explaining the sustained efforts devoted to the development of efficient systems for selective Ac(III) separations. For instance, it was demonstrated that phosphoric acid derivatives and N-containing compounds, such as malonamide, succinamide, glutalamide or glycolamide ligands, are efficient chelating species for trivalent actinides (see Figure 3).^{16,142,143} However, in the case of the malonamide-based ligands significant amounts of fission products, such as Eu(III), Zr(IV), and Fe(III), can also be co-extracted with Ac(III), making these ligands less favorable for industrial applications. Interestingly, bicyclic malonamides were shown to interact much more strongly than their linear counterparts and often showed better separation factors. First, as an example of immobilized P-based ligands, phosphonic acid-grafted mesoporous silica sorbents were proven to be efficient sorbents for capturing highly toxic radionuclides with long half-lives like ^{241}Am .¹⁴⁴ The results exposed fast adsorption rate of Am(III) with equilibrium reached in less than 10 min and no apparent changes in K_d values were seen after 30 min for all samples studied. In addition, this work suggests an influence of the mesostructure of the silica sorbent (*e.g.*, SBA-15, MCM-41 and PMO-type material) and functionalization degree on the adsorption performance. Especially, the authors observed that the functionalized SBA-15 sorbent with the highest amount of functional groups (P content around 1.6 mmol g^{-1}) possesses the highest Am uptake ($K_d = 0.39 \text{ L g}^{-1}$) while the lowest sorption of Am was observed for the modified MCM-41 material (with the ligand content about 0.9 mmol g^{-1}), K_d being 0.20 L g^{-1} . Concerning N-based ligands for Ac(III), most of the studies so far were still mostly concerned with their properties in liquid-liquid extraction methods. In general, the glycolamide ligands showed higher binding efficiency towards Ac(III) and Ac(IV) in acidic waste solutions than malonamide ligands.¹⁴⁵ Studies concerning the development of malonamide and

diamide ligands, for solvent extraction purposes, and investigation of the structures of extractant-Ln or -Ac complexes have shown that the extractability of diglycolamide (DGA) for actinides is higher than that of malonamide (MA). In addition, the ether oxygen in DGA plays an important role in the chelation process with the actinides. On the other hand, the length of the alkyl chain attached to the N atom of the amide group controls the distribution ratios between Ac(III) and Ln(III) and the solubility of the amide in the organic phase.¹⁴⁶ Only very recently, Nitsche and co-workers¹⁴⁷ showed that DGA-functionalized mesoporous SBA-15 silica may actually be effective for the extraction of americium ions from aqueous solutions at pH 3-4. However, although the tridentate ligands, *e.g.*, diglycolamide have increased affinities for trivalent actinides, they also exhibit significant uptakes for lanthanides (Ln). Consequently, DGA-functionalized silica materials have recently been used by several different groups for lanthanide separation.^{38,126,147,148,149} In general, the DGA-based ligands have drawn much more attention as very effective ligands for the complexation of f-elements with better separation factor for lanthanides and, therefore these ligand systems will be discussed in the following section.

Solid-phase sorbents used for REE separation

Most of the sorbents developed for REE separation are functionalized with well-known ligands used in LLE applications. Efficient chelating ligands containing phosphorous, tertiary amine coupled with either carboxylic or ester moieties, and amide-based groups (see Figure 3) have been reported for this task. These moieties have been anchored through (post-synthesis) grafting strategies onto several solid-phase supports, such as ordered mesoporous silica materials (*e.g.*, KIT-6, SBA-15, MCM-41),^{16,38,42,126,150,151,152} microspheres,⁴⁴ nanoparticles,^{149,153} monoliths⁴⁵ or metal oxide nanoparticles (*e.g.*, Fe₃O₄, TiO₂).^{154,155} Fewer attempts have been performed on carbon-based supports, such as mesoporous carbon¹⁵⁶ or graphene oxide.^{157,158} Some researchers have also studied the application of simple un-functionalized^{141,157}

or oxidized-only supports, however, both types of sorbents usually lack the required selectivity for REE separation/purification or showed insufficient analyte uptake.¹⁵⁶ Therefore, they were not included in this review. A list of the most common ligands and supports used for REE solid-phase separation is given in Table 3.

Phosphorous-based ligands

Although the phosphorous-based ligands are mostly used for Ac extraction as described previously, their role as efficient chelates for REEs has also been widely explored.^{42,151,154,159,160} These ligands are used principally in the final purification step, where the individual metals are isolated from a mixture of elements. Several organophosphorous ligands were reported in the literature and demonstrated good sorption behavior. This list of ligands includes organophosphoric acid, phosphonic acid $\text{PO}(\text{OH})_2$ and phosphonic ester $\text{PO}(\text{OR})_2$ -based derivatives (see Figure 3).^{42,151,154,159,160}

Several metal oxides functionalized with phosphonic acid moieties have demonstrated good performance for the extraction of lanthanides. For instance, it was shown that porous mixed metal oxide functionalized with tris-methylenephosphonic acid displayed high extraction capacity for Gd^{3+} ions (K_d values above 1×10^4), where un-functionalized support demonstrated negligible affinity to Gd^{3+} .¹⁵⁹ Veliscek-Carolan et al.¹⁶⁰ showed that porous zirconium organophosphonate materials (prepared from zirconium propoxide and varying amounts of amino tris-methylenephosphonic acid) exhibits also high Eu extraction capacity, being 40 mg g^{-1} in average. Moreover, for materials with higher $\text{P}/(\text{P}+\text{Zr})$ molar ratios, the K_d values observed for the targeted elements (*e.g.*, La, Nd, Eu, Ho, Yb) were much higher than for other competing elements (*e.g.*, Co, Ce, Sr), however, no selectivity among REEs was observed. On the other hand, slightly better selectivity profile was observed for materials with lower $\text{P}/(\text{P}+\text{Zr})$ molar ratios, *i.e.*, selectivity towards lighter elements from La to Eu.

In case of the silica supports, the most common phosphorous ligands, such as phosphonic acid¹⁵¹ or phosphoric ester⁴² derivatives, are introduced on the surface by grafting the respective commercially-available silanes (refluxing in dry toluene). Among phosphorous-containing silica sorbents, the materials containing phosphonic acid usually displayed better capacity and affinity towards lanthanides. For instance, Fryxell and co-workers⁴² tested their SAMMS modified with phosphonic acid and phosphonic ester functionalities for Ln extraction. The authors showed that in case of the ester-modified material, a significant retention of competing ions (*i.e.*, Fe, Ni, Cu, Zn, K, Ca) was noticeable ($K_d(\text{Eu}) = 260 \text{ mL g}^{-1}$, $K_d(\text{Fe}) = 1800 \text{ mL g}^{-1}$), however, the acid-functionalized SAMMS material showed no significant sorption of non-targeted elements, such as transition metals or alkaline earth metal cations. In particular, significant competition between iron ions and the lanthanides was observed with the ester-modified SAMMS sorbent, in which the ligand forms a 6-membered ring chelate with the metal cation favoring the complexation of the transition metals. Hence, the ester ligand shows a modest affinity for the smaller and more acidic Fe(III). The acid-SAMMS sorbent did not display this tendency, exhibiting little competitive process with the transition or alkaline earth metal cations. The affinity, reusability, extraction capacity and kinetics of lanthanide sorption from natural waters and acidic solutions using SAMMS materials functionalized with diphosphonic acid, acetamide phosphonic acid, propionamide phosphonic acid and 1-hydroxy-2-pyridinone were also investigated.¹⁵¹ Depending on the pH of the extraction medium and the type of ligand grafted, different selectivities towards REEs were observed. Nonetheless, the materials exhibited very fast metal uptake reaching over 95 % after 1 minute for Gd and 99 % after 10 minutes. Moreover, the regenerable character of the SAMMS sorbents following loading/elution cycles (6) was also demonstrated. Interestingly, the kinetic profile of activated carbon, which was used as comparison guide with the modified SAMMS materials, was much slower, *i.e.*, approximately 15% of Gd was adsorbed by the activated carbon after 24 h.¹⁵¹ According to these authors, the rapid Gd uptake presented by the SAMMS materials was due to the rigid structure and suitable pore sizes of the silica sorbents which

facilitate the access of metal species to the binding sites located inside the pores. Furthermore, in a comparative study, SAMMS sorbents displayed slightly faster metal uptake than microspheres-based counterpart. The difference in adsorption rates of these materials was attributed to the different pore size of the sorbents (3.5 - 4.5 nm for the SAMMS compared to 2.2 nm for the microspheres) or to the various density of the functional groups (1.4 mmol g⁻¹ compared to 0.9 mmol g⁻¹, respectively).¹⁵¹

Nitrogen-containing ligands

Another industrially important class of ligands for lanthanide separation are the amino-based compounds and among them, the most often used are quaternary ammonium salts, known for instance as Aliquat 336[®]. The extraction mechanism of such compounds mostly relies on anion exchange process. The selectivity of Aliquat 336[®] extractant is diverse and depends on the extraction medium used. For example, Aliquat 336[®] displays selectivity towards lighter lanthanides in presence of nitrates, but a shifted selectivity towards heavier elements in presence of thiocyanate.¹⁶¹ In order to obtain a pure elemental fraction, quaternary ammonium salts are usually mixed with additional complexing agents such as ethylenediaminetetraacetic acid (EDTA) or diethylenetriaminepentaacetic acid (DTPA). EDTA,^{154,162} iminodiacetic acid (IDAA)¹⁶ or glycinilurea silane Gly-UR⁴² ligands have been grafted on silica supports and their performance in solid-phase systems appeared very promising. For instance, according to the data reported by Dupont et al.,¹⁵⁵ EDTA-functionalized silica nanoparticles display higher Gd³⁺ uptake than functionalized metal oxide nanoparticles, such as TiO₂ or Fe₃O₄. The average uptake of smaller rare earth elements follows this order: SiO₂-EDTA > TiO₂-EDTA > Fe₃O₄-EDTA, essentially caused by the increasing amounts of ligands on the surface of these nanoparticles (50, 36 and 15 wt. %, respectively). The stripping of lanthanide ions from the nanoparticles was found to be very efficient (98 %) and expeditious, typically in less than 5 minutes. Moreover, the selectivity of EDTA-functionalized nanoparticles was tested from the concentrated solutions of two metals, *i.e.*, La and Eu. From these experiments, it appears that density

of the EDTA functionalities influences greatly the selectivity. For instance, increasing amount of the EDTA functions resulted in the materials being more selective towards smaller element, such as Er^{3+} , while lower amounts of ligand favored larger ions, such as La^{3+} .¹⁵⁵ According to the authors, this phenomenon is related to the reduction of the “cage” size of the EDTA ligand, limited when high densities of EDTA groups are present on the surface of the nanoparticles, as well as potential steric hindrance. Moreover, higher enrichment factors (*i.e.*, separation factor, SF) were observed for $\text{La}^{3+}/\text{Lu}^{3+}$ (SF = 4) than for $\text{La}^{3+}/\text{Pr}^{3+}$ (SF = 2) (see Figure 8) as a result of the marked differences in ionic radius.

The nitrogen-containing ligands, such as iminodiacetic acid (IDA)⁴¹ or tripodal nitroxide ligand,² such as tris(2-*tert*-butylhydroxy-aminato)benzylamine (H_3TriNOx), have also been successfully applied for Nd/Dy purification. For instance, Kessler et al.⁴¹ studied the uptake capacity of Dy, Nd and La ions by iminodiacetic acid-functionalized magnetic nanoparticles coated with a silica layer. The IDA ligand was obtained by the condensation of iodopropyl triethoxysilane and iminodiacetic acid dimethyl ester. The thus-prepared sorbent revealed a slightly higher capacity towards the heavier lanthanides with reported capacities of 40 mg g^{-1} for Dy^{3+} and only about 28 mg g^{-1} for La^{3+} . The enrichment factors for the Dy/Nd and Dy/La metals in the case of adsorption from pH-neutral solutions were reported at approximately 4:1. Desorption at lower pH (pH = 3) greatly impacted the Dy/La separation factor ratio (81:1). This pH-dependent desorption can be foreseen as selective and efficient separation method. According to the authors, the Dy/La separation is based on differences in the mode of coordination in the respective metal complex formed. In case of Dy ions, the metal complex has centrosymmetric triclinic structure with octa-coordinated Dy ions. The coordination sphere of Dy ions includes 8 oxygen atoms: four atoms from the IDA ligands, two from coordinated nitrates and last two oxygen atoms from coordinated water molecules (Figure 9). Differently, the La^{3+} complex showed more orthorhombic structure. The La atoms are deca-coordinated by the 2 chelating carboxylate groups, 2 oxygen atoms of bridging carboxylate groups, 4 oxygen atoms of coordinated water molecules and the nitrate anions are not involved in the coordination

sphere (non-coordinated counter-ions). High extraction capacities were also reported for DTPA ligand attached to Stöber-type nanoparticles prepared by the co-condensation of silica precursors and chitosan.¹⁶² Here, it was shown that the DTPA-functionalized sorbent quantitatively adsorbs Nd^{3+} from the extraction solution, while EDTA-sorbent adsorbed only a portion of the present ions (80 %). Interestingly, the equilibration time was reached faster in the case of the DTPA-sorbent than the EDTA-based material (2 vs. 3 h). Roosen et al.¹⁶² investigated in details the recycling and enrichment factor between dysprosium and neodymium for both sorbents in batch and dynamic systems at relatively low pH (1-2). In the case of batch extraction, both materials showed an enrichment factor Dy/Nd equal to 2 at pH 2. Decrease in pH values resulted in an increased Dy/Nd separation factor exceeding 3 for DTPA-chitosan-silica sorbent. Thus, the DTPA-chitosan-silica material showed a higher selectivity than EDTA-chitosan-silica sorbent towards adsorption of dysprosium (III) in comparison with neodymium (III). Further, it was observed that HNO_3 solution (pH 1) is necessary to desorb neodymium from the column, while at this pH dysprosium stayed 'immobilized' on the column, and thus, both elements could be effectively separated. The dysprosium ions were stripped by elution with 1 M nitric acid. In addition, the reusability studies showed that these resins could be reused for other separation experiments, however, 15 % adsorption efficiency drop was observed after the first recycling cycle.

Extraction behavior and Ac/Ln separation factors in the liquid-liquid system of nitrogen-based ligands, such as malonamide (MA), succinamide (SCA), maleamide (MLA), diglycolamide (DGA) and oxydipropionamide (ODPA) (see Figure 3) were investigated by Sasaki and co-workers.¹⁴⁶ The extraction results carried out in nitric acid showed, in addition to the higher extraction capacity, selectivity for heavy elements (HREEs) for the DGA ligand, while the rest of the ligands displayed similar or slightly higher distribution factors for lighter REEs (LREEs). The iminodiacetamide-silane (IDA) SAMMS sorbents synthesized by the Fryxell team showed good extraction properties with distinct kinetic profiles ($\text{Lu}^{3+} > \text{Eu}^{3+} > \text{Gd}^{3+} > \text{Nd}^{3+} > \text{Ce}^{3+}$).¹⁵⁰ These authors postulated that a dense monolayer of the IDA ligand and

high surface area with open pore structure could explain the high binding capacity and rapid sorption kinetics observed. Surprisingly, even if aprotic chelating ligands are relatively attractive for transition metals or alkaline earth cations, studies from mixture of competing elements showed no sign of competitive adsorption in presence of alkaline earth cations and only modest sorption of transition metal cations (*e.g.*, Mn and Ni).¹⁵⁰ Furthermore, IDA-amide SAMMS materials displayed rather little affinity for the lanthanide cations at pH below 5, mostly because of the protonation of the N atom. Thus, much higher affinity towards Ln was reported under neutral conditions (pH \approx 6.5).

Recently, the diamide ligands were adapted as extractants in the SLE sorbents. For instance, the DGA derivatives combined with an acrylic ester matrix, Amberchrom-CG71, are commercially produced as normal DGA Resin (TODGA) and branched DGA Resin (TEHDGA) (Eichrom Technologies Inc.).^{28,163} Both of the resins showed higher uptake of HREEs than LREEs, which is in agreement with the behavior observed in LLE experiment with these ligands. For these commercial sorbents, equilibrium was reached within 10 minutes and the extraction capacity for trivalent elements was an order of magnitude higher than for TRU resin (extractant system is octylphenyl-N,N-di-isobutyl carbamoylphosphine oxide dissolved in TBP). Moreover, in comparison to the TRU resin,^{28,163} the DGA resins showed the uptake of U(VI) was greatly suppressed, while the uptake of Am(III) was significantly enhanced relative to Th(IV) and Pu(IV). It is documented that the DGA ligand is complexing trivalent metal ions through two carbonyl oxygen donors and an ether oxygen donor forming two stable five-membered chelate rings and represents approximately a 3:1 stoichiometry (Figure 10).¹⁶⁴

Most recently, these DGA-type ligands were introduced on mesoporous silica surfaces via grafting procedures. The initial attempt was reported by Florek and co-workers in 2014³⁸ who efficiently functionalized KIT-6 silica with a designed diglycolamide-silane. Following this work, Zheng and collaborators reproduced¹⁴⁹ this system by attaching a similar ligand to the silica support, but this time using an approach based on maleic anhydride chemistry. Corroborating the results published by Florek

et al.³⁸, the materials synthesized by Zheng and co-workers¹⁴⁹ demonstrated greater selectivity for SEG (*i.e.*, Gd). Lower uptake for other competing elements and high degree of reusability over a 5 cycles were also reported. In general, good extraction performance in low pH (4) was observed by our team with the DGA-modified materials.^{38,126,148} In this case, focus was placed on the importance of the grafting procedure used for the sorbent synthesis (Figure 11). For instance, it was evidenced that various grafting protocols of the same chelating ligand can provide different extraction performance of the final materials.³⁸ A material where the ligand was grafted in a two-step sequence (noted as KIT-6-N-DGA-2) displayed much lower extraction capacity and lower selectivity than a material functionalized in one-step using a modified silane (material noted as KIT-6-N-DGA-1) (Figure 11). In case of the two-step functionalization, in the first step, the amino-propyl chain was attached to the silica surface followed by reaction with diglycolyl chloride. Differently, a modified silane was prepared by solution reaction of aminopropyltriethoxysilane with diglycolyl chloride and the resulting bridged DGA-disilane molecule was grafted in one-step on the silica surface. The better extraction behavior of the material modified in one-step may be attributed to a more rigid structure of the ligand that is fixed to the silica support. In contrast, the two-step grafting leads to mixture of different functionalities, such as ligand units that are attached to the surface from one or both sides, as well as some residual (un-modified) amino moieties (Figure 11). Interestingly, KIT-6-N-DGA-1 showed high selectivity towards mid-size lanthanides and very low uptake of competing elements, such as Fe, Al, U or Th ions. On the other hand, the commercial DGA resin, tested in the same extraction conditions, did not show such interesting Ln selectivity and displayed much higher extraction capacity for competing elements than to targeted ions. Following this first success, we also varied the synthesis of the DGA-chelating ligand and generated a family of derivatives, such as FDGA (furan-2,4-diamidopropyltriethoxysilane) and DOODA (3,6-dioxaoctanediamido-propyltriethoxysilane) ligands, which exhibited different *bite angle* (that is, the angle between the ligand coordination sites and the metal center) compared to previously synthesized DGA-ligand (Figure 12). Here, it was presumed that by

adjusting the structural parameters of the DGA ligand, *i.e.*, by slight modification of the relative position of the oxygen atoms in the DGA backbone, diverse separation abilities and different metal selectivities could be achieved. Consequently, larger ions would favor binding to a ligand with a larger *bite angle* whereas smaller metals would prefer binding ligands with smaller angle. Indeed, it was shown that the REE selectivity can be altered depending on the ligand tethered to the silica support, its geometry and environment. For instance, in comparison to the initial KIT-6-N-DGA-1, the sorbent modified with DOODA ligand (KIT-6-N-DOODA) revealed higher selectivity to the heavier lanthanides (Ho-Lu), in agreement with a smaller *bite angle* of this ligand, *i.e.*, smaller *bite angle* between ligand and La was observed for La-DOODA (57.90-58.27°) compared to La-DGA complexes (60.35-60.93°) (Figures 12 and 13). Differently, the KIT6-N-FDGA sorbent did not display particular selectivity towards lanthanides but revealed an interesting high selectivity for scandium.¹⁴⁸ Furthermore, the extraction performance of these solid sorbents was also compared directly with the corresponding LLE systems where the same ligands were used. This comparison emphasized that by careful modification of the *bite angle* of organic moieties and by imparting rigidity to the ligand, *i.e.*, grafting on a surface, a more selective extraction of lanthanides could be achieved than in the liquid-liquid phase system.¹⁴⁸ Importantly, tetraoctyl(TO)DGA in LLE showed higher selectivity for smaller lanthanides, while in contrast, the solid-state DGA equivalent system was more efficient for extracting middle lanthanides. This opposite behavior of the same ligand in different environments could be attributed to lower flexibility of the ligand when chemically anchored on the mesopore surface. Thus, immobilizing of a ligand seems to provide a more stable *bite angle* yielding a more pronounced selectivity towards selected REE cations. However, further investigations including molecular modelling and spectroscopic study of the coordination environments, will be needed to fully answer the question of the role of the ligand *bite angle*, which will then pave the way for the design of new and highly selective ligand systems.

Another interesting study was performed by Awual et al.⁴⁵ who used large cage-like mesoporous silica monolith for separation/recovery of trace lanthanides (Nd, Eu and Yb ions) from wastewater streams with N-octyl-N-tolyl-1,10-phenanthroline-2-carboxamide (HA)-modified sorbents. The Langmuir adsorption model revealed adsorption capacity of about 176, 163, and 162 mg g⁻¹ for Yb, Eu and Nd ions, respectively. However, in the presence of the co-existing cations, *i.e.*, Al³⁺, the sorption capacity towards targeted elements was strongly impacted, *i.e.*, between 21-31 % of decrease in sorption was observed when aluminum ions were present in the extraction solution. In addition, after each extraction cycle, the sorption capacity slightly decreased and after eight cycles the decrease was significant (from 170 to approximately 130 mg g⁻¹ for Nd and from 170 to about 150 mg g⁻¹ for Yb). These materials reached the adsorption equilibrium within short time, *i.e.*, 98 % sorption efficiency was observed after 50 min for Yb, 60 min for Eu and 70 min for Nd ions, respectively. The authors postulated that the metal interactions in liquid state with O- and N-donors, such as in the complexes, are nearly the same as lanthanide coordination in the solid state version. Moreover, EXAFS data revealed that O and N atoms of the HA ligand are strongly coordinated to the lanthanide ions and form stable complexes, where the lanthanide and ligand ratio was found to be 1:2. As proposed by the authors, the interaction mechanism of different metals, *i.e.*, Nd, Eu, Yb, seems to depend on the ionic radii of these elements and their complexation ability. In agreement with Florek and co-workers,¹⁴⁸ immobilization of the ligand on a solid monolithic support decreases the flexibility of the ligands, thus the mobility of the ligand is considered negligible and its *bite angle* is less flexible. Due to the smaller ionic radii of Yb compared to the two other elements, the coulombic interaction between Yb ions and the ligands were presumed to be greater than that in case of Eu and Nd ions resulting in the observed higher Yb selectivity.

Conclusion and outlook

Despite the development of modern hydrometallurgical extractions procedures, efficient separation and purification of actinides and rare earth elements still remains as tedious and challenging task. In order to produce pure elemental fraction, multiple separation steps are typically required owing to the similarities in chemical properties of these elements. These separations are usually performed in commercial ventures by liquid-liquid extraction. Nevertheless, current solvent extraction developments are still insufficient to meet the economic expectations and environmental restrictions associated with such activities. Due to reduction of solvent consumption and minimization of waste produced, the liquid-solid extraction process presents a commercially interesting alternative. Unfortunately, this alternative approach is nonetheless plagued by several issues, such as limited extraction capacity, low radiance stability and lack of reusability. Many of these issues could be overcome through the development of solid-phase extraction. Among the different SPE materials reported in the literature, ordered mesoporous silica and carbon materials appear as promising candidates for the replacement of present LLE and SLE extractions approaches. The possibility of pore size tuning combined with a great variety of particle size and shape and the relative facility to perform functionalization of the surface, make mesoporous silica materials one of the best candidates as solid-phase sorbents. In addition, significant extraction capacities, good selectivities and adequate reusability of such silica-based materials can be regarded as good indicators of their potential performances in environmental remediation technologies and critical resource recovery processes without the need of multiple purification steps. Yet, several issues still need to be addressed, for instance, the limited stability of silica-based sorbents in very acidic/basic conditions or the permeability and pressure-drop problems encountered in the dynamic systems. In case of pressure limitation, the use of mesoporous-macroporous monolithic structures seems to be a promising avenue. On the other hand, when dealing with pH stability, carbon-based sorbents can be helpful, as they usually possess higher chemical resistance, although carbon functionalization is more challenging than for silica materials. Therefore, it can be hypothesized that, within the current knowledge, the optimal sorbent could

be carbon monoliths. Beside the choice of an appropriate solid support, the selection of the ligand and the grafting procedure should be thoroughly debated prior to sorbent development. Unfortunately, despite comprehensive information reported in the literature, very often the real working capacity of mesoporous sorbents or clear comparison between different systems cannot be easily done. The difficulties are caused mostly because of a lack of standardized extraction requirements and procedures. Although several techniques can be used for sorbent characterization, only few research groups perform fully detailed extraction studies. Most often, research papers show only extraction capacities calculated in the 'ideal' conditions, *i.e.*, when no competing elements are present in the extraction solution or in optimal pH conditions. Furthermore, the reported experiments often describe only batch extraction methods and do not deal with dynamic (flow-through) extraction systems, while the later procedure is generally used in industrial applications. Clearly, there is a great need for guidelines and recommendations that should be always followed in order to allow unambiguous assessment of the extraction performance of solid-phase (mesoporous) sorbents. Among them, we recommend the measurement of complete adsorption isotherms, as well as providing kinetic and reusability studies, which should be viewed as mandatory information. In addition, the influence of the additional/competing elements and pH variation should be verified. Moreover, in case of the sorbents designed for separation of radioactive species, the irradiation stability should be discussed and, when possible, tested. Furthermore, it could also be interesting to provide tabulated figure of merits as a tool to standardize the qualification of the solid sorbents analytical performances. That is, for instance, extraction capacity in the range: 0-20 mg g⁻¹ as moderate sorbent; 20-50 mg g⁻¹ as acceptable sorbent; 50-100 mg g⁻¹ as excellent sorbent; above 100 mg g⁻¹ as outstanding. Similarly, this approach could be used to qualify extraction time: *i.e.*, equilibration time below 3 min, outstanding extraction rate; 3-10 min, excellent extraction rate, 10-30 min acceptable extraction rate; and above 1 h moderate extraction rate.

From the literature review, it appears that phosphorous-based sorbents are more suitable for actinide separation (*i.e.*, uranium extraction), while nitrogen-containing ligands seems to more suitable for the lanthanide separation, in particular amide-based functions. Nevertheless, the choice of the ligand is often determined by several factors, including the type of the metal source, the chemical composition of the separation mixture, the presence/absence of competing elements and the final application. Furthermore, the chemical structure of the ligand can be modified by adding bulky groups or carbon atoms, *i.e.*, by tuning of the ligand *bite angle*, and consequently the selectivity of the synthesized materials can be altered. In addition, typical REEs or Ac sources are a mixture of several different elements, *i.e.*, targeted elements, transition metals, alkali metals and radioactive species. Accordingly, effective sorbents should contain highly selective ligands that have high preference towards targeted species with low affinity for other elements. High selectivity combined with high extraction capacity should reduce the number of steps needed for the metal purification, and therefore, be beneficial for the industrial applications as well as been advantageous for an environmental perspective. The specificity of the ligand is also an important issue, since very often the concentration of REEs or Ac is much lower than other competing metals, *i.e.*, Al, Fe, or alkali metal ions; making the separation process even more difficult and tedious.

Acknowledgements

The authors acknowledge the Fonds de Recherche Québécois Nature et Technologies (FRQNT) and National Sciences and Engineering Research Council of Canada (NSERC) for financial support. The Natural Sciences and Research Council of Canada supported this work through a Strategic Project Grant.

References

- 1 N. Tzanetakis and K. Scott, *J. Chem. Technol. Biotechnol.*, 2004, **79**, 919-926.
- 2 J. A. Bogart, C. A. Lippincott, P. J. Carroll and E. J. Schelter, *Angew. Chem. Int. Ed.*, 2015, **54**, 8222-8225.
- 3 Nuclear Safety Review for the Year 2014; International Atomic Energy Agency: Vienna, Austria, 2014.
- 4 L. R. Anspaugh, R. J. Catlin and M. Goldman, *Science*, 1988, **242**, 1513-1519.
- 5 G. Brumfiel, *Nature*, 2011, **472**, 146-147.
- 6 S. Massari and M. Ruberti, *Res. Policy*, 2013, **38**, 36-43.
- 7 Critical raw materials for the EU, *Report of the Ad-hoc Working Group on defining critical raw materials*, 2010.
- 8 U.S. Department of Energy, Critical materials strategy,
http://energy.gov/sites/prod/files/DOE_CMS2011_FINAL_Full.pdf, (accessed November 2015).
- 9 E. Alonso, A. M. Sherman, T. J. Wallington, M. P. Everson, F. R. Field, R. Roth and R. E. Kirchain, *Environ. Sci. Technol.*, 2012, **46**, 3406-3414.
- 10 S. Cotton, *Lanthanide and Actinide Chemistry*, ed. John Wiley & Sons, Ltd., Wiley, 2006.
- 11 L. Sherrington, *Commercial processes for rare earths and thorium*, in: *Handbook of Solvent Extraction*, ed. M.H.I. Baird, C. Hanson, Wiley, New York, 1983, pp. 717-723.
- 12 Y. Kanazawa and M. Kamitani, *J. Alloys. Compd.*, 2006, **408-412**, 1339-1343.
- 13 D. Hart and D. Lush, *The chemical toxicity potential of CANDU spent fuel*, report # 631.22904.101, NWMO, 2004.
- 14 B. Kronholm, C. G. Anderson and P. R. Taylor, *JOM*, 2013, **65**, 1321-1326.
- 15 I. McGill, *Rare Earth Elements*, in: *Ullmann's Encyclopedia of Industrial Chemistry*, ed. Wiley-VCH, Weinheim, 2000, 183-228.
- 16 a) B. E. Johnson, P. H. Santschi, C.-Y. Chuang, S. Otsuka, R. S. Addleman, M. Douglas, R. D. Rutledge, W. Chouyok, J. D. Davidson, G. E. Fryxell and J. M. Schwantes, *Environ. Sci. Technol.*, 2012, **46**, 11251-11258; b) A. Leoncini, P. K. Mohapatra, A. Bhattacharyya, D. R. Raut, A. Sengupta, P. K. Verma, N. Tiwari, D. Bhattacharyya, S. Jha, A. M. Wouda, J. Huskens and W. Verboom; *Dalton Trans.*, 2016, **45**, 2476-2484; c) A. Sengupta, P. K. Mohapatra, A. B. Patil, R. M. Kadam and W. Verboom; *Sep. Purif. Technol.*, 2016, **162**, 77-83; d) Y. Fang, X. Yuan, L. Wu, Z. Peng, W. Feng, N. Liu, D. Xu, S. Li, A. Sengupta, P. K. Mohapatra and L. Yuan, *Chem. Commun.*, 2015, **51**, 4263-4266.
- 17 P. Anastas and N. Eghbali, *Chem. Soc. Rev.*, 2010, **39**, 301-312.
- 18 P. T. Anastas and J. B. Zimmerman, *Environ. Sci. Technol.*, 2003, **37**, 94A-101A.

- 19 *Principle and Practices of Solvent Extraction Principles and Practice, Revised and Expanded*, ed. J. Rydberg, M. Cox, C. Musikas and G. R. Choppin, Marcel Dekker 2nd, ed. New York, Inc., 2004.
- 20 Y. Sasaki, Y. Tsubata, Y. Kitatsuji, Y. Sugo, N. Shirasu, Y. Morita and T. Kimura, *Solvent Extr. Ion Exch.*, 2013, **31**, 401-415.
- 21 X. Wang, W. Li and D. Li, *J. Rare Earths*, 2011, **29**, 413-415.
- 22 V. Petrenko and A. Siinmaa, *Process flow sheet*, in *Turning a Problem into a Resource: Remediation and Waste Management at the Sillamäe Site, Estonia*, ed. C. K. Rofer, T. Kaasik, Springer Science & Business Media, 2000, 47-56.
- 23 D. Melzner, J. Tilkowski, A. Mohrmann, W. Poppe, W. Halwachs and K. Schügerl, *Hydrometallurgy*, 1984, **13**, 105-123.
- 24 a) R. Renner, *Environ. Sci. Technol.*, 2001, **35**, 410A-413A; b) I. Billard, A. Ouadi and C. Gaillard, *Anal. Bioanal. Chem.*, 2011, **400**, 1555-1566; c) A. Bhattacharyya, S. A. Ansari, T. Gadly, S. K. Ghosh, M. Mohapatra and P. K. Mohapatra, *Dalton Trans.*, 2015, **44**, 6193-6201.
- 25 X. Sun, H. Luo and S. Dai, *Dalton Trans.*, 2013, **42**, 8270-8275.
- 26 X. Sun and K. E. Waters, *ACS Sustainable Chem. Eng.*, 2014, **2**, 1910-1917.
- 27 D. Larivière, T. A. Cumming, S. Kiser, C. Li and R. J. Cornett, *J. Anal. At. Spectrom.*, 2008, **23**, 352-360.
- 28 E. P. Horwitz, R. Chiarizia, M. L. Dietz, H. Diamond and D. M. Nelson, *Anal. Chim. Acta.*, 1993, **281**, 361-372.
- 29 a) A. R. Türker, *Sep. Purif. Rev.*, 2012, **41**, 169-206; b) T. J. Tranter, *Solid-phase extraction technology for actinide and lanthanide separations in nuclear fuel reprocessing*, in *Advanced Separation Techniques for Nuclear Fuel Reprocessing and Radioactive Waste Treatment*, ed. K.L. Nash, G.L. Lumetta, Woodhead Publishing Series in Energy, 2011, pp. 377-413.
- 30 J. Li, X. Yang, C. Bai, Y. Tian, B. Li, S. Zhang, X. Yang, S. Ding, C. Xia, X. Tan, L. Ma and S. Li, *J. Colloid Interface Sci.*, 2015, **437**, 211-218.
- 31 G. J. A. A. Soler-Illia, C. Sanchez, B. Lebeau and J. Patarin, *Chem. Rev.*, 2002, **102**, 4093-4138.
- 32 X. S. Zhao, G. Q. Lu and G. J. Millar, *Ind. Eng. Chem. Res.*, 1996, **35**, 2075-2090.
- 33 D. Zhao, J. Sun, Q. Li and G. D. Stucky, *Chem. Mater.*, 2000, **12**, 275-279.
- 34 R. E. Subden, R. G. Brown and A. C. Noble, *J. Chromatogr. A*, 1978, **166**, 310-312.
- 35 S. L. C. Ferreira, H. M. C. Andrade and H. C. dos Santos, *J. Colloid Interface Sci.*, 2004, **270**, 276-280.
- 36 P. J. Lebed, J.-D. Savoie, J. Florek, F. Bilodeau, D. Larivière and F. Kleitz, *Chem. Mater.*, 2012, **24**, 4166-4176.

- 37 S. Schneider, A. Caldas Garcez, M. Tremblay, F. Bilodeau, D. Larivière and F. Kleitz, *New J. Chem.*, 2013, **37**, 3877-3880.
- 38 J. Florek, F. Chalifour, F. Bilodeau, D. Larivière and F. Kleitz, *Adv. Funct. Mater.*, 2014, **24**, 2668-2676.
- 39 M. Choi and J. Jang, *J. Colloid Interface Sci.*, 2008, **325**, 287-289.
- 40 Y. Zhao, J. Li, S. Zhang and X. Wang, *RSC Adv.*, 2014, **4**, 32710-32717.
- 41 E. P. Legaria, S. D. Topel, V. G. Kessler and G. A. Seisenbaeva, *Dalton Trans.*, 2015, **44**, 1273-1282.
- 42 G. E. Fryxell, H. Wu, Y. Lin, W. J. Shaw, J. C. Birnbaum, J. C. Linehan, Z. Nie, K. Kemner and S. Kelly, *J. Mater. Chem.*, 2004, **14**, 3356-3363.
- 43 Y. Wei, J. Qian, L. Huang and D. Hua, *RSC Adv.*, 2015, **5**, 64286-64292.
- 44 I. V. Melnyk, V. P. Goncharyk, L. I. Kozhara, G. R. Yurchenko, A. K. Matkovsky, Y. L. Zub and B. Alonso, *Microporous Mesoporous Mater.*, 2012, **153**, 171-177.
- 45 M. R. Awual, T. Kobayashi, H. Shiwaku, Y. Miyazaki, R. Motokawa, S. Suzuki, Y. Okamoto and T. Yaita, *Chem. Eng. J.*, 2013, **225**, 558-566.
- 46 B. C. Luo, L. Y. Yuan, Z. F. Chai, W. Q. Shi and Q. Tang, *J. Radioanal. Nucl. Chem.*, 2016, **307**, 269-276.
- 47 X. Zhao, M. Wong, C. Mao, T. X. Trieu, J. Zhang, P. Feng and X. Bu, *J. Am. Chem. Soc.*, 2014, **136**, 12572-12575.
- 48 a) J. Park, Z. U. Wang, L.-B. Sun, Y.-P. Chen and H.-C. Zhou, *J. Am. Chem. Soc.*, 2012, **134**, 20110-20116; b) S. M. Cohen, *Chem. Rev.*, 2012, **112**, 970-1000; c) F.A. Almeida Paz, J. Klinowski, S.M. F. Vilela, J.P.C. Tomé, J.A. S. Cavaleiro and J. Rocha, *Chem. Soc. Rev.*, 2012, **41**, 1088-1110.
- 49 A. Walcarius and L. Mercier, *J. Mater. Chem.*, 2010, **20**, 4478-4511.
- 50 J. S. Beck, J. C. Vartuli, W. J. Roth, M. E. Leonowicz, C. T. Kresge, K. D. Schmitt, C. T. W. Chu, D. H. Olson and E. W. Sheppard, S. B. McCullen, J. B. Higgins, and J. L. Schlenker, *J. Am. Chem. Soc.*, 1992, **114**, 10834-10843.
- 51 D. Zhao, Q. Huo, J. Feng, B. F. Chmelka and G. D. Stucky, *J. Am. Chem. Soc.*, **1998**, **120**, 6024-6036.
- 52 F. Kleitz, S. H. Choi and R. Ryoo, *Chem. Commun.*, 2003, 2136-2137.
- 53 A. Galarneau, J. Iapichella, D. Brunel, F. Fajula, Z. Bayram-Hahn, K. Unger, G. Puy, C. Demesmay and J. L. Rocca, *J. Sep. Sci.*, 2006, **29**, 844-855.
- 54 R. Tian, J. Sun, H. Zhang, M. Ye, C. Xie, J. Dong, J. Hu, D. Ma, X. Bao and H. Zou, *Electrophoresis*, 2006, **27**, 742-748.
- 55 T. Martin, A. Galarneau, F. Di Renzo, D. Brunel and F. Fajula, *Chem. Mater.*, 2004, **16**, 1725-1731.
- 56 L. B. McCusker, *Rev. Mineral. Geochem.*, 2005, **57**, 1-16.

- 57 S. Mann, S. L. Burkett, S. A. Davis, C. E. Fowler, N. H. Mendelson, S. D. Sims, D. Walsh and N. T. Whilton, *Chem. Mater.*, 1997, **9**, 2300-2310.
- 58 B. Smarsly, S. Polarz and M. Antonietti, *J. Phys. Chem. B*, 2001, **105**, 10473-10483.
- 59 E. Krämer, S. Förster, C. Göltner and M. Antonietti, *Langmuir*, 1998, **14**, 2027-2031.
- 60 A. P. Wight and M. E. Davis, *Chem. Rev.*, 2002, **102**, 3589-3614.
- 61 A. Sayari and S. Hamoudi, *Chem. Mater.*, 2001, **13**, 3151-3168.
- 62 H. Yoshitake, *New J. Chem.*, 2005, **29**, 1107-1117.
- 63 D. M. Ford, E. E. Simanek and D. F. Shantz, *Nanotechnology*, 2005, **16**, S458-S475.
- 64 F. Hoffmann, M. Cornelius, J. Morell and M. Fröba, *Angew. Chem. Int. Ed.*, 2006, **45**, 3216-3251.
- 65 Y. Lin, G. E. Fryxell, H. Wu and M. Engelhard, *Environ. Sci. Technol.*, 2001, **35**, 3962-3966.
- 66 G. E. Fryxell, S. V. Mattigod, Y. Lin, H. Wu, S. Fiskum, K. Parker, F. Zheng, W. Yantasee, T. S. Zemanian, R. S. Addleman, J. Liu, K. Kemner, S. Kelly and X. Feng, *J. Mater. Chem.*, 2007, **17**, 2863-2874.
- 67 P. Makowski, X. Deschanel, A. Grandjean, D. Meyer, G. Toquer and F. Goettmann, *New J. Chem.*, 2012, **36**, 531-541.
- 68 D. Zhao, J. Feng, Q. Huo, N. Melosh, G. H. Fredrickson, B. F. Chmelka and G. D. Stucky, *Science*, 1998, **279**, 548-552.
- 69 M. Kruk, M. Jaroniec, C. H. Ko and R. Ryoo, *Chem. Mater.*, 2000, **12**, 1961-1968.
- 70 (a) F. Kleitz, *Ordered Microporous and Mesoporous Materials*, in *Nanoscale Materials in Chemistry*, John Wiley & Sons 2 ed., 2009, Ch. 9, pp. 243-329; (b) F. Kleitz, F. Bérubé, R. Guillet-Nicolas, C.-M. Yang, M. Thommes, *J. Phys. Chem. C*, 2010, **114**, 9344-9355.
- 71 Y. Wan and D. Zhao, *Chem. Rev.*, 2007, **107**, 2821-2860.
- 72 N. Hiyoshi, K. Yogo and T. Yashima, *Microporous Mesoporous Mater.*, 2005, **84**, 357-365.
- 73 G. J. A. A. Soler-Illia, E. L. Crepaldi, D. Grosso and C. Sanchez, *Curr. Opin. Colloid Interface Sci.*, 2003, **8**, 109-126.
- 74 T. Amatani, K. Nakanishi, K. Hirao and T. Kodaira, *Chem. Mater.*, 2005, **17**, 2114-2119.
- 75 C. G. Brown and L. G. Sherrington, *J. Chem. Technol. Biotechnol.*, 1979, **29**, 193-209.
- 76 C.-M. Yang, W. Schmidt and F. Kleitz, *J. Mater. Chem.*, 2005, **15**, 5112-5114.
- 77 N. V. Reichhardt, R. Guillet-Nicolas, M. Thommes, B. Klösgen, T. Nylander, F. Kleitz and V. Alfredsson, *Phys. Chem. Chem. Phys.*, 2012, **14**, 5651-5661.
- 78 H. Staub, R. Guillet-Nicolas, N. Even, L. Kayser, F. Kleitz and F.-G. Fontaine, *Chem. Eur. J.*, 2011, **17**, 4254-4265.

- 79 M. Ide, M. El-Roz, E. De Canck, A. Vicente, T. Planckaert, T. Bogaerts, I. Van Driessche, F. Lynen, V. Van Speybroeck, F. Thybault-Starzyk and P. Van Der Voort, *Phys. Chem. Chem. Phys.*, 2013, **15**, 642-650.
- 80 Y.-L. Wang, L. Zhu, B.-L. Guo, S.-W. Chen and W. S. Wu, *New J. Chem.*, 2014, **38**, 3853-3861.
- 81 J. L. Vivero-Escoto, M. Carboni, C. W. Abney, K. E. deKrafft and W. Lin, *Microporous Mesoporous Mater.*, 2013, **180**, 22-31.
- 82 X. Wang, G. Zhu and F. Guo, *Annals. Nuclear Energy*, 2013, **56**, 151-157.
- 83 Y. Meng, D. Gu, F. Zhang, Y. Shi, H. Yang, Z. Li, C. Yu, B. Tu, D. Zhao, *Angew. Chem. Int. Ed.* 2005, **44**, 7053-7059.
- 84 S. Tanaka, N. Nishiyama, Y. Egashira and K. Ueyama, *Chem. Commun.*, 2005, 2125-2127.
- 85 C. Liang, Z. Li and S. Dai, *Angew. Chem. Int. Ed.*, 2008, **47**, 3696-3717.
- 86 R. Ryoo, S. H. Joo and S. Jun, *J. Phys. Chem. B*, 1999, **103**, 7743-7746.
- 87 R. Ryoo, S. H. Joo, M. Kruk and M. Jaroniec, *Adv. Mater.*, 2001, **13**, 677-681.
- 88 A. Thomas, F. Goettmann and M. Antonietti, *Chem. Mater.*, 2008, **20**, 738-755.
- 89 A. Taguchi, J. H. Smått and M. Lindén, *Adv. Mater.*, 2003, **15**, 1209-1211.
- 90 H. Zhong and Q. Yang, *Monolithic chromatography and its modern applications*, ed. P. G. Wang, St. Albans, ILM, 2010, Ch. 3, pp. 59-78.
- 91 J. Liu, T. Y. Yang, D.-W. Wang, G. Q. Lu, D. Zhao and S. Z. Qiao, *Nature Commun.*, 2013, **4**, 2798.
- 92 Y. Zhai, Y. Dou, D. Zhao, P. F. Fulvio, R. T. Mayes and S. Dai, *Adv. Mater.*, **2011**, **23**, 4828-4850.
- 93 T. Parsons-Moss, H. Tüysüz, D. Wang, S. Jones, D. Olive and H. Nitsche, *Radiochim. Acta.*, 2014, **102**, 489-504.
- 94 Y. F. Yue, X. G. Sun, R. T. Mayes, J. Kim, P. F. Fulvio, Z. A. Qiao, S. Brown, C. Tsouris, Y. Oyola and S. Dai, *Sci. China. Chem.*, 2013, **56**, 1510-1515.
- 95 M. Carboni, C. W. Abney, K. M. L. Taylor-Pashow, J. L. Vivero-Escoto and W. Lin, *Ind. Eng. Chem. Res.*, 2013, **52**, 15187-15197.
- 96 D. T. T. Nguyen, D. Guillarme, S. Rudaz and J. L. Veuthey, *J. Sep. Sci.*, 2006, **29**, 1836-1848.
- 97 E. L. Pfaunmiller, M. L. Paulemond, C. M. Dupper and D. S. Hage, *Anal. Bioanal. Chem.*, 2013, **405**, 2133-2145.
- 98 P. Coufal, Z. Bosáková, J. Širc, V. Pacáková and K. Štulík, *Monolithic chromatography and its modern applications*, ed. P. G. Wang, ILM, St. Albans, 2010, Ch. 4, pp. 79-100.
- 99 Y. Yue, R. T. Mayes, J. Kim, P. F. Fulvio, X.-G. Sun, C. Tsouris, J. Chen, S. Brown and S. Dai, *Angew. Chem. Int. Ed.*, 2013, **52**, 13458-13462.
- 100 K. Nakanishi and N. Soga, *J. Am. Ceram. Soc.*, 1991, **74**, 2518-2530.

- 101 Y. Sato, K. Nakanishi, K. Hirao, H. Jinnai, M. Shibayama, Y. B. Melnichenko and G. D. Wignall, *Colloids Surf. A.*, 2001, **187–188**, 117-122.
- 102 K. Nakanishi, T. Amatani, S. Yano and T. Kodaira, *Chem. Mater.*, 2008, **20**, 1108-1115.
- 103 J.H. Smått, S. Schunk and M. Lindén, *Chem. Mater.*, 2003, **15**, 2354-2361.
- 104 K. Nakanishi, Y. Sato, Y. Ruyat and K. Hirao, *J. Sol-Gel Sci. Technol.*, 2003, **26**, 567-570.
- 105 H. Maekawa, J. Esquena, S. Bishop, C. Solans and B. F. Chmelka, *Adv. Mater.*, 2003, **15**, 591-596.
- 106 M. J. Yoo and D. S. Hage, *Monolithic chromatography and its modern applications*, ed. P. G. Wang, ILM, St. Albans, 2010, Ch. 1, pp. 3-26.
- 107 S. E. Mourabit, M. Guillot, G. Toquer, J. Cambedouzou, F. Goettmann and A. Grandjean, *RSC Adv.*, 2012, **2**, 10916-10924.
- 108 M.V. Landau, S.P. Varkey, M. Herskowitz, O. Regev, S. Pevzner, T. Sen and Z. Luz, *Microporous Mesoporous Mater.*, 1999, **33**, 149-163.
- 109 X. Yang, J. Li, J. Liu, Y. Tian, B. Li, K. Cao, S. Liu, M. Hou, S. Li and L. Ma, *J. Mater. Chem. A*, 2014, **2**, 1550-1559.
- 110 Z. B. Zhang, X.-F. Yu, X.-H. Cao, R. Hua, M. Li and Y.-H. Liu, *J. Radioanal. Nucl. Chem.*, 2014, **301**, 821-830.
- 111 B. Hu, K. Wang, L. Wu, S. H. Yu, M. Antonietti and M.-M. Titirici, *Adv. Mater.*, 2010, **22**, 813-828.
- 112 M.-M. Titirici and M. Antonietti, *Chem. Soc. Rev.*, 2010, **39**, 103-116.
- 113 F. Becker and B. Kienzler, *Open. Chem.*, 2015, **13**, 586-590.
- 114 P. J. Lebed, K. de Souza, F. Bilodeau, D. Larivière and F. Kleitz, *Chem. Commun.*, 2011, **47**, 11525-11527.
- 115 W. Yantasee, Y. Lin, G.E. Fryxell and Z. Wang, *Electroanal.*, 2004, **16**, 870-873.
- 116 J. R. Kumar, J.-S. Kim, J.-Y. Lee, and H.-S. Yoon, *Sep. Purif. Rev.*, 2011, **40**, 77-125.
- 117 J. N. Mathur, M. S. Murali and K. L. Nash, *Solvent Extr. Ion Exch.*, 2001, **19**, 357-390.
- 118 J. N. Mathur, M. S. Murali, P. R. Natarajan, L. P. Badheka, A. Banerji, A. Ramanujam, P. S. Dhami, V. Gopalakrishnan, R. K. Dhumwad and M. K. Rao, *Waste Manage.*, 1993, **13**, 317-325.
- 119 E. P. Horwitz and D. G. Kalina, *Solvent Extr. Ion Exch.*, 1984, **2**, 179-200.
- 120 J. N. Mathur, M. S. Murali P. R. Natarajan, L.P. Badheka and A. Banerji, *Talanta*, 1992, **39**, 493-496.
- 121 K. Hatakeyama, Y.-Y. Park, H. Tomiyasu and Y. Ikeda, *J. Nucl. Sci. Technol.*, 1995, **32**, 1146-1153.
- 122 E. P. Horwitz, H. Diamond and K. A. Martin, *Solvent Extr. Ion Exch.*, 1987, **5**, 447-470.
- 123 C. Z. Wang, J. H. Lan, Y. L. Zhao, Z. F. Chai, Y. Z. Wei and W.Q. Shi, *Inorg. Chem.*, 2013, **52**, 196-203.

- 124 E. P. Horwitz, M. L. Dietz, R. Chiarizia, H. Diamond, S. L. Maxwell III and M. R. Nelson, *Anal. Chim. Acta.*, 1995, **310**, 63-78.
- 125 K. Vidya, S. E. Dapurkar, P. Selvam, S. K. Badamali and N. M. Gupta, *Microporous Mesoporous Mater.*, 2001, **50**, 173-179.
- 126 E. Juère, J. Florek, D. Larivière, K. Kim and F. Kleitz, *New J. Chem.*, 2016, DOI: 10.1039/C5NJ03147H.
- 127 L.-Y. Yuan, Y.-L. Liu, W.-Q. Shi, Y.-L. Lv, J.-H. Lan, Y.-L. Zhao and Z. F. Chai, *Dalton Trans.*, 2011, **40**, 7446-7453.
- 128 W. Zhang, G. Ye and J. Chen, *J. Mater. Chem. A*, 2013, **1**, 12706-12709.
- 129 G. E. Fryxell, Y. Lin, S. Fiskum, J. C. Birnbaum, H. Wu, K. Kemner and S. Kelly, *Environ. Sci. Technol.*, 2005, **39**, 1324-1331.
- 130 F. Endrizzi, A. Melchior, M. Tolazzin and L. Rao, *Dalton Trans.*, 2015, **44**, 13835-13844.
- 131 S.-H. Choi and Y. C. Nho, *Radiat. Phys. Chem.*, 2000, **57**, 187-193.
- 132 S. Katragadda, H. D. Gesser and A. Chow, *Talanta*, 1997, **45**, 257-263.
- 133 Y.-Y. Park, S.-Y. Kim, J.-S. Kim, M. Harada, H. Tomiyasu, M. Nogami and Y. Ikeda, *J. Nucl. Sci. Technol.*, 2000, **37**, 344-348.
- 134 S. Vukovic, L. A. Watson, S. O. Kang, R. Custelcean and B. P. Hay, *Inorg. Chem.*, 2012, **51**, 3855-3859.
- 135 C. Gunathilake, J. Górka, S. Dai and M. Jaroniec, *J. Mater. Chem. A*, 2015, **3**, 11650-11659.
- 136 N. Mehio, B. Williamson, Y. Oyola, R. T. Mayes, C. Janke, S. Brown and S. Dai, *Ind. Eng. Chem. Res.*, 2015, DOI: 10.1021/acs.iecr.5b03211.
- 137 N. Mehio, M. A. Lashely, J. W. Nugent, L. Tucker, B. Correia, C.-L. Do-Thanh, S. Dai, R. D. Hancock and V. S. Bryantsev, *J. Phys. Chem. B*, 2015, **119**, 3567-3576.
- 138 L. Huang, L. Zhang and D. Hua, *J. Radioanal. Nucl. Chem.*, 2015, **305**, 445-453.
- 139 J. Geng, L. J. Ma, H. Wang, J. Liu, C. Y. Bai, Q. Song, J. Li, M. Hou and S. J. Li, *J. Nanosci. Nanotechnol.*, 2012, **12**, 7354-7363.
- 140 S. Xie, X. Liu, B. Zhang, H. Ma, C. Ling, M. Yu, L. Li and J. Li, *J. Mater. Chem. A*, 2015, **3**, 2552-2558.
- 141 Y. Wang, Z. Gu, J. Yang, J. Liao, Y. Yang, N. Liu and J. Tang, *Appl. Surf. Sci.*, 2014, **320**, 10-20.
- 142 S. Sharma, S. Panja, A. Bhattachariya, P. S. Dhama, P. M. Gandhi and S. K. Ghosh, *Dalton Trans.*, 2015, **44**, 12771-12779.
- 143 H. Wu, Q. Y. Wu, C. Z. Wang, J. H. Lan, Z. R. Liu, Z. F. Chaia and W. Q. Shi, *Dalton Trans.*, 2015, **44**, 16737-16745.
- 144 W. Zhang, X. He, G. Ye, R. Yi, and J. Chen, *Environ. Sci. Technol.*, 2014, **48**, 6874-6881.
- 145 Y. Sasaki and G. R. Choppin, *Radiochim. Acta.*, 1998, **80**, 85-88.

- 146 Y. Sasaki and S. Tachimori, *Solvent Extr. Ion. Exch.*, 2002, **20**, 21-34.
- 147 J. A. Shusterman, H. E. Mason, J. Bowers, A. Bruchet, E. C. Uribe, A. B. Kersting and H. Nitsche, *ACS Appl. Mater. Inter.*, 2015, **7**, 20591–20599.
- 148 J. Florek, A. Mushtaq, D. Larivière, G. Cantin, F.-G. Fontaine and F. Kleitz, *RSC Adv.*, 2015, **5**, 103782-103789.
- 149 X. Zheng, C. Wang, J. Dai, W. Shi and Y. Yan, *J. Mater. Chem. A*, 2015, **3**, 10327-10335.
- 150 G. E. Fryxell, W. Chouyyok and R. D. Rutledge, *Inorg. Chem. Commun.*, 2011, **14**, 971-974.
- 151 W. Yantasee, G. E. Fryxell, R. S. Addleman, R. J. Wiacek, V. Koonsiripaiboon, K. Pattamakomsan, V. Sukwarotwat, J. Xu and K. N. Raymond, *J. Hazard. Mater.*, 2009, **168**, 1233-1238.
- 152 M. R. Awual, M. M. Hasan, A. Shahat, M. Naushad, H. Shiwaku and T. Yaita, *Chem. Eng. J.*, 2015, **265**, 210-218.
- 153 S. D. Topel, E. P. Legaria, C. Tiseanu, J. Rocha, J.-M. Nedelec, V. G. Kessler and G. A. Seisenbaeva, *J. Nanopart. Res.*, 2014, **16**, 2783-2799.
- 154 M. P. Moloney, J. Causse, C. Loubat and A. Grandjean, *Eur. J. Inorg. Chem.*, 2014, **2014**, 2268-2277.
- 155 D. Dupont, W. Brullot, M. Bloemen, T. Verbiest and K. Binnemans, *ACS Appl. Mater. Inter.*, 2014, **6**, 4980-4988.
- 156 T. Parsons-Moss, J. Wang, S. Jones, E. May, D. Olive, Z. Dai, M. Zavarin, A. B. Kersting, D. Zhao and H. Nitsche, *J. Mater. Chem. A*, 2014, **2**, 11209-11221.
- 157 Y. Sun, Q. Wang, C. Chen, X. Tan and X. Wang, *Environ. Sci. Technol.*, 2012, **46**, 6020-6027.
- 158 H. Chen, D. Shao, J. Li and X. Wang, *Chem. Eng. J.*, 2014, **254**, 623-634.
- 159 C. S. Griffith, M. De Los Reyes, N. Scales, J. V. Hanna and V. Luca, *ACS Appl. Mater. Inter.*, 2010, **2**, 3436-3446.
- 160 J. Veliscek-Carolan, T. L. Hanley and V. Luca, *Sep. Purif. Technol.*, 2014, **129**, 150-158.
- 161 J. S. Preston and A. C. Du Preez, *Solvent extraction processes for the separation of rare earth metals*, in *Solvent Extraction*, ed. T. Sekine, Elsevier, pp. 883-894.
- 162 J. Roosen, J. Spoooren and K. Binnemans, *J. Mater. Chem. A*, 2014, **2**, 19415-19426.
- 163 E. P. Horwitz, D. R. McAlister, A. H. Bond and R. E. Barrans, *Solvent Extr. Ion. Exch.*, 2005, **23**, 319-344.
- 164 K. Matloka, A. Gelis, M. Regalbuto, G. Vandegrift and M. J. Scott, *Dalton Trans.*, 2005, **23**, 3719-3721.

Table 1 Compilation of the most common ligands and supports used for Ac solid-phase separation (n.a. - not analyzed, ^{Cal} - Calculated maximum adsorption capacity from the Langmuir model).

Ligand type	Support	Element	Extraction conditions			Performance		Re-cycling (No cycles)	Ref
			pH	Time	Competitive elements	K _d (ml g ⁻¹)	Capacity (mg g ⁻¹)		
Alkyl phosphine oxides	Vinyl co-condensed mesoporous silica	U	0.5 - 6	24 h	n.a.	n.a.	100	n.a.	128
Phosphoric acid	Commercial mesoporous carbon	U	4 - 8.2	0-1 h	n.a.	n.a.	96.8 ^{cal} - 67.1 ^{cal}	n.a.	95
	Mesoporous silica	U	1.5 - 8	0-4 h	n.a.	n.a.	2380 ^{cal}	n.a.	127
DPTS	KIT-6 SBA-15	U	4	0-30 min	Multi-element solution (27 elements)	10200 4200	n.a.	n.a.	114
	KIT-6 SBA-15	U	4	0-30 min	n.a.	n.a.	55 ^{Cal} 49 ^{Cal}	5 n.a.	36
	Mesoporous copolymer	U	8	0-30 days	Seawater	n.a.	1.99	n.a.	99
	Mesoporous silica	U	8	24 h	n.a.	n.a.	57.3	n.a.	134
Amidoxime	Polyamidoxime functionalized nanoparticles	U	4 - 12	0-10 h	n.a.	n.a.	246.9 ^{cal}	5	138
	Polymer coated mesoporous carbon	U	8	24 h	n.a.	29977	62.7	n.a.	94
	Nanofibrous polymers composite	U	8	24 h	V, Fe, Co, Ni, Cu, Zn, Pb, Mg, and Ca	n.a.	1.5	n.a.	140
	Multiwalled carbon nanotubes	U	1 - 4.5	0-4 h	Mn, Co, Ni, Zn, Sr, Ba and Cs	840	176 ^{cal}	n.a.	141
Amidoxime / Poly amonium	Poly (styrene/divinyl benzene)-functionalized microspheres	U	3-8	0-35h	K, Ni, Cu, Zn, Pb	3654	169.5 ^{cal}	n.a.	43
-	CMK-8 Oxidized CMK-8	Pu	1 - 10	0-6 days	n.a.	n.a.	9.4 - 9.6	n.a.	93

Table 2 Characteristic of mesoporous silica sorbents and their extraction performance. Adapted with permission from reference [36]. Copyrights 2012 ACS.

Support	Ligand	Surface area ($\text{m}^2 \text{g}^{-1}$)	Pore size ^a (nm)	V_{pore} ($\text{cm}^3 \text{g}^{-1}$)	Weight ^b loss (%)	q_m^c (mg g^{-1})
KIT-6-100	DPTS	614	7.9	0.92	5.2	54
SBA-15-100	DPTS	635	7.9	0.92	5.2	51

^a) Results obtained from physisorption of N_2 at 77K, NLDFT adsorption branch kernel.

^b) Calculated from the onset temperature to 560 °C.

^c) Calculated maximum adsorption capacity from the Langmuir model.

Table 3 Compilation of most common ligands and supports used for REEs solid-phase separation (n.a. -not analyzed, (a) Trismethylenephosphonic acid, (b) Diethylphosphatoethyltriethoxysilane, (c) Malonamide).

Ligand type	Support	Extracted Element	Extraction conditions			Performance		Re-cycling (No cycles)	Ref
			pH	Time (h)	Competitive elements	K_d (ml g ⁻¹)	Capacity max (mg g ⁻¹)		
ATMP ^{a)}	Metal oxide (Zr)	La, Nd, Eu, Ho, Yb	0.1M HNO ₃	24	Co, Cs, Sr	n.a.	30-60 (Eu)	n.a.	160
	Metal oxide (ZrTi)	Gd	0-3M HNO ₃	0-24	n.a.	10145	0.8	n.a.	159
DPETE ^{b)}	Silica microspheres	Nd, Dy	5.8 (Nd) 4.8 (Dy)	1	n.a.	n.a.	43 (Nd) 49 (Dy)	2	44
Ac-Phos Prop-Phos	Silica SAMMS [®]	La, Nd, Eu, Lu	1-8	2	Fe, Ni, Cu, Zn, K, Ca	0-400000	n.a.	1-10	42, 151
H ₂ IDA	Core shell γ -Fe ₂ O ₃ @SiO ₂	La, Nd, Dy	n.a.	0-50	n.a.	n.a.	28 (La) 34 (Nd) 40 (Dy)	n.a.	41
DGA	KIT-6	REEs	4	0.5	Al, Fe, U, Th	7000 (Eu)	n.a.	5	38
FDGA	KIT-6	REEs	4	0.5	Al, Fe, U, Th	11000 (Sc)	75(Eu)	10	148
DOODA	KIT-6	REEs	4	0.5	Al, Fe, U, Th	5000 (Er-Lu)	75(Eu)	10	148
HA	Silica monoliths	Nd, Eu, Yb	1-5.4	0 - 1.3	Na, K, Ca, Mn, Al	n.a.	162 (Nd) 163 (Eu) 176 (Yb)	8	45
MA ^{c)}	Silica NP	Sm-Er	4	0 - 4.2	Al, Fe	2673 (Gd)	85.4 (Gd)	5	149
EDTA	Chitosan Silica	La, Nd, Eu, Dy, Lu	1-7	0-6	n.a.	n.a.	61(Nd)	4	162
DTPA	Chitosan Silica	La, Nd, Eu, Dy, Lu	1-7	0-6	n.a.	0-350	107 (Nd)	4	162

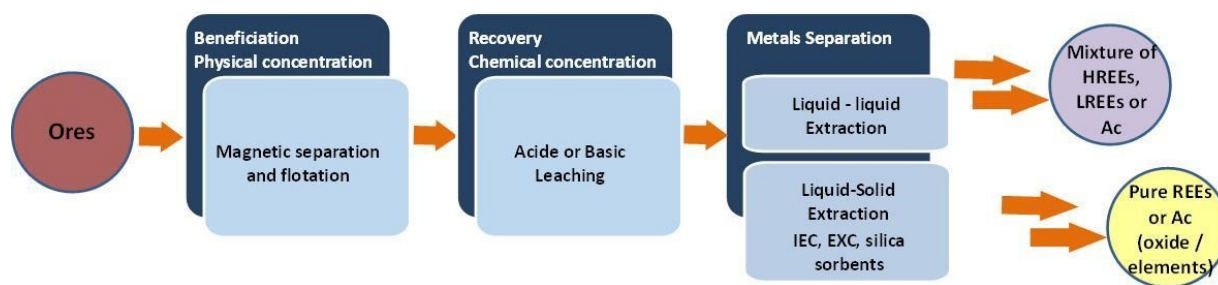


Figure 1 Simplified schematic representation of REE and Ac extraction process (see text for acronym definitions).

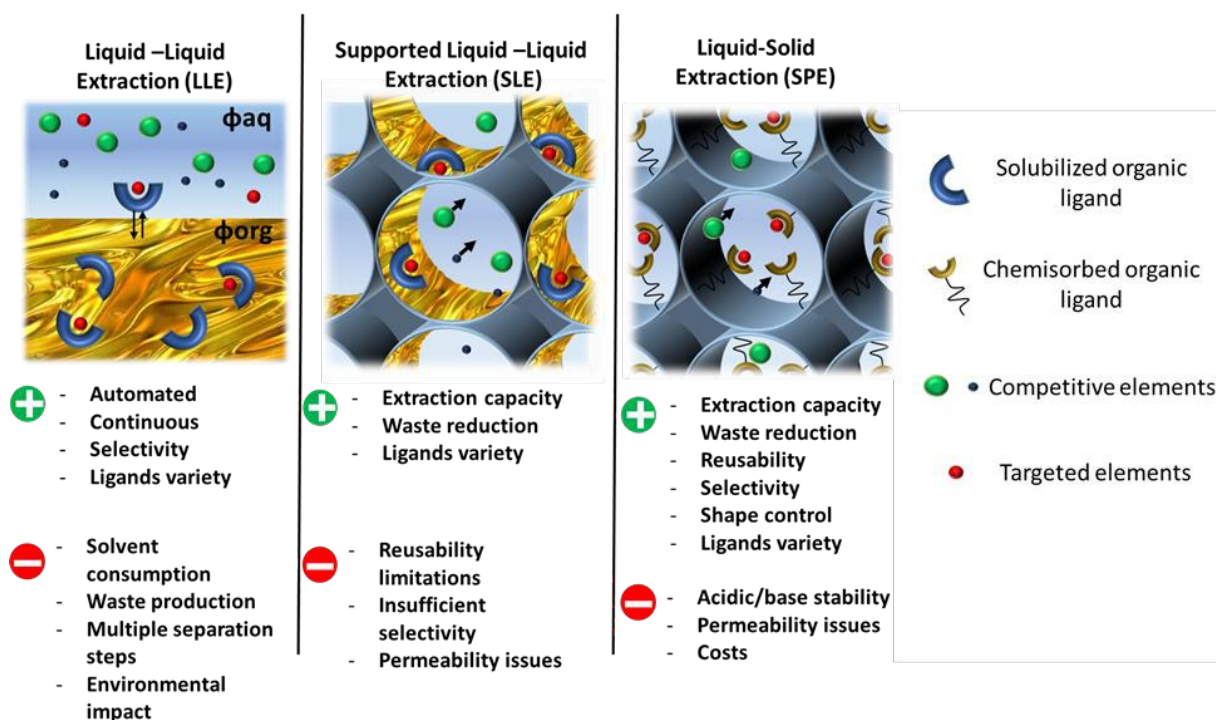


Figure 2 Comparison between liquid-liquid (LLE) and liquid-solid (SLE, SPE) extraction methods.

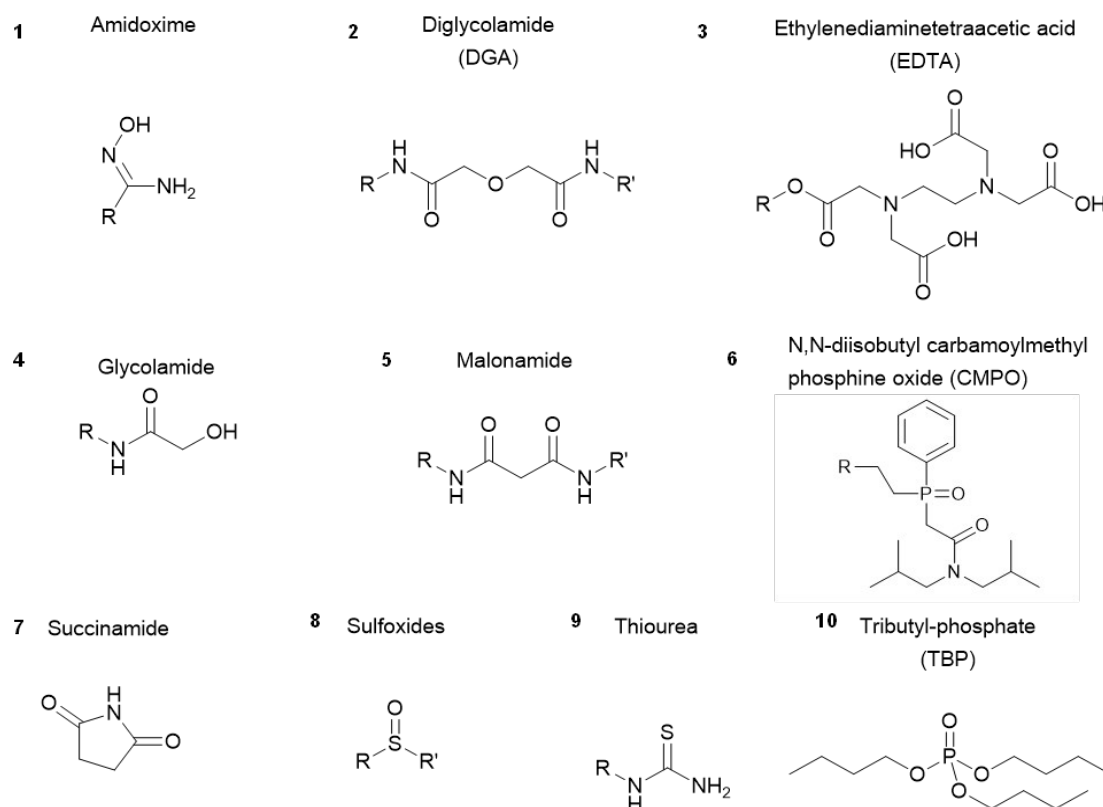


Figure 3 Types of ligands which are most commonly used for actinide and lanthanide separation.

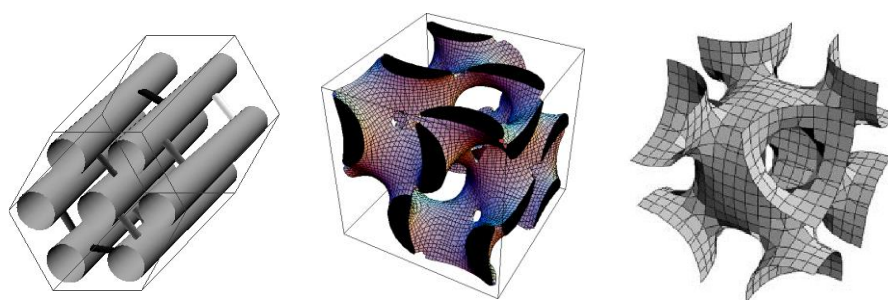


Figure 4 Schematic representations of the mesostructure of typical mesoporous solid supports (e.g., SBA-15, KIT-6 and SBA-16, from left to right). Reproduced with permission from reference [70a]. Copyrights 2009 Wiley.

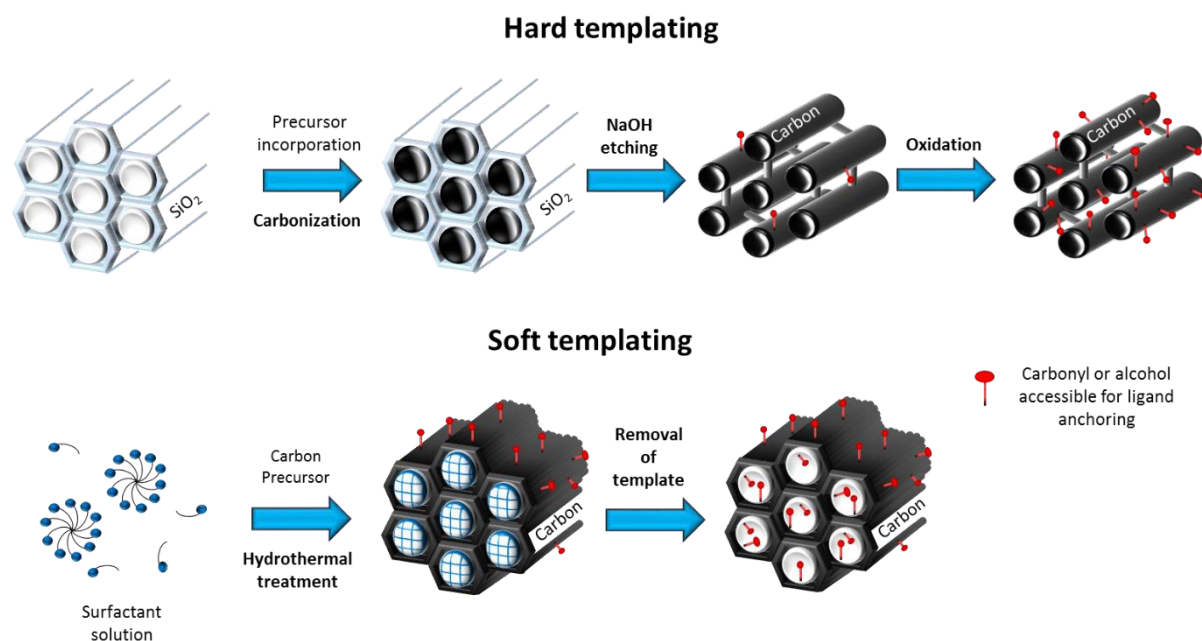


Figure 5 Synthesis of nanoporous carbon by hard templating and soft templating methods.

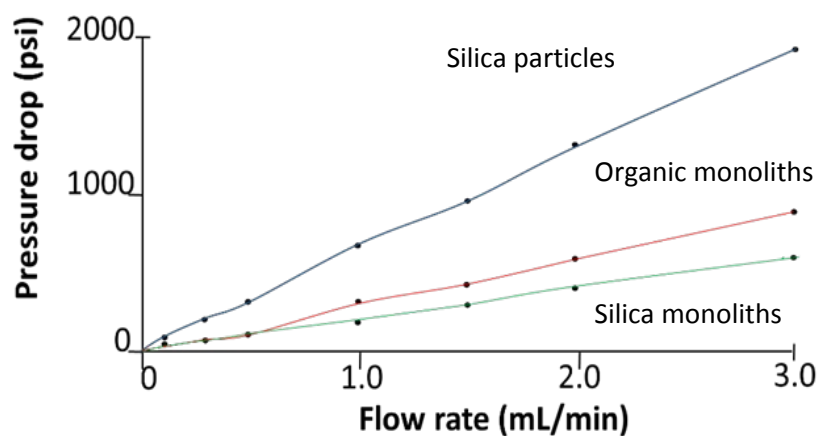


Figure 6 Comparison of the pressure drop for the silica particles and monoliths-based columns. Reproduced with permission from reference [97]. Copyrights 2013 Springer.

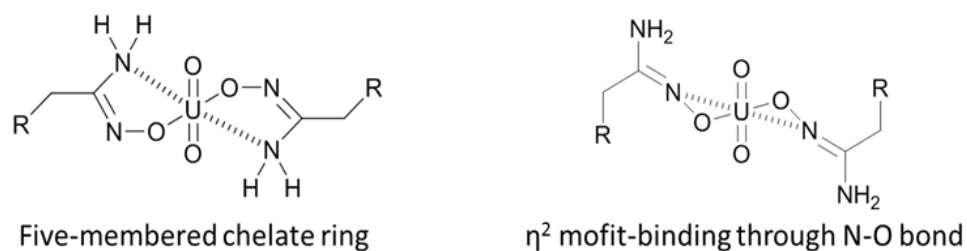


Figure 7 Possible chelating interactions of the amidoxime ligand and uranium ions. Reproduced with permission from reference [135]. Copyrights 2015 RSC.

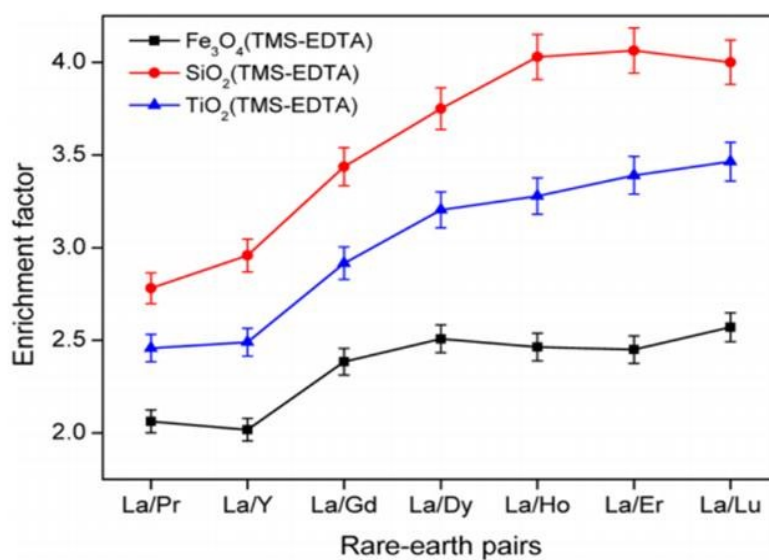


Figure 8 Separation factors between La³⁺ and other III-valence lanthanides with increasing difference in the ionic radii. Reproduced with permission from reference [155]. Copyrights 2014 ACS.

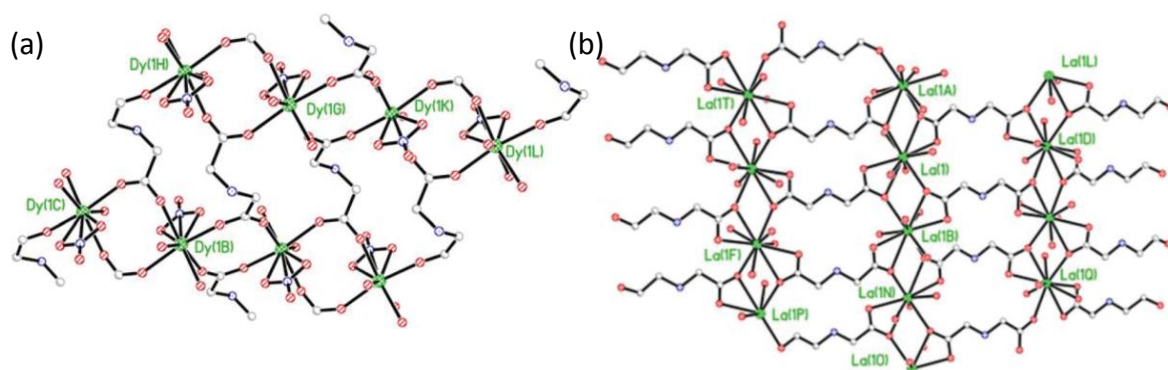


Figure 9 IDA complexes with different REEs: (a) Dy and (b) La. Reproduced with permission from reference [41]. Copyrights 2015 RSC.

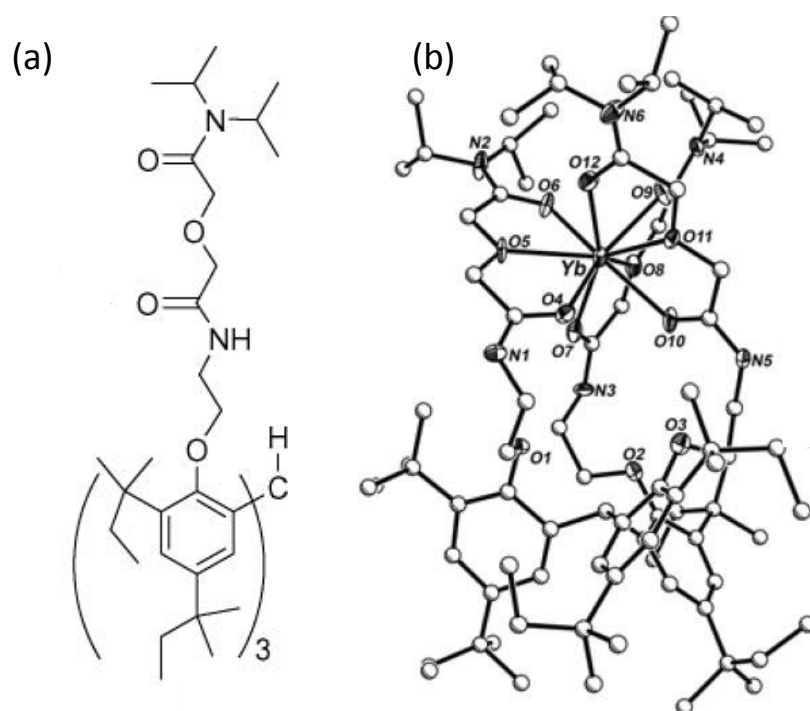


Figure 10 Complexation of the derivative of diglycolamide (DGA) ligand (a) and structures of the DGA-Yb complex Yb (b). Reproduced with permission from reference [164]. Copyrights 2005 RSC.

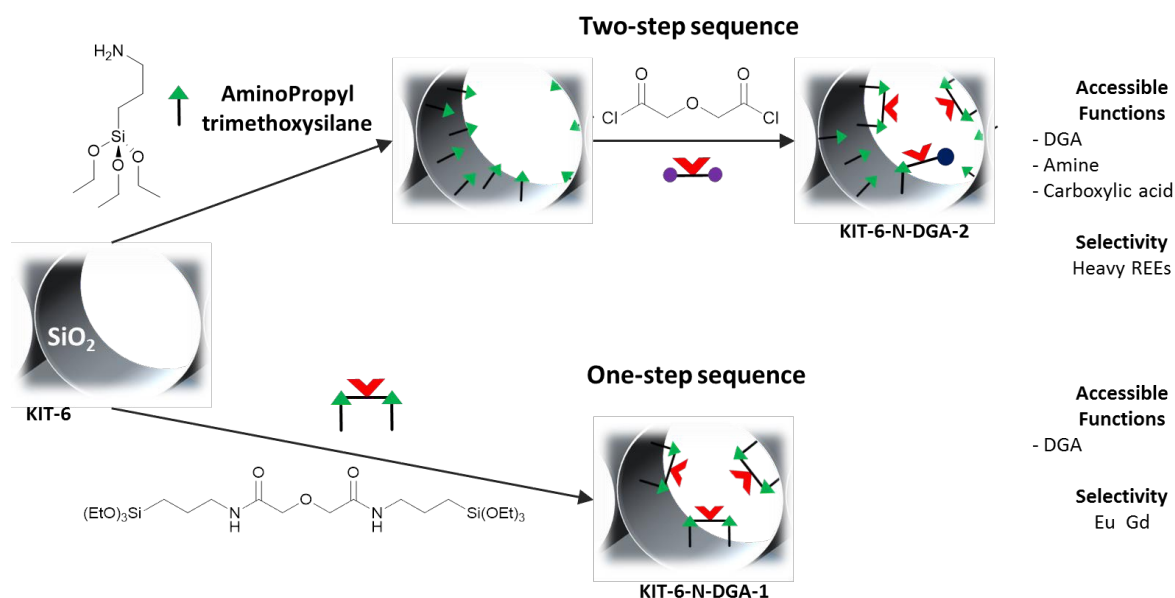


Figure 11 Schematic representation of the two- and one-step DGA grafting procedures. Adapted with permission from reference [38]. Copyrights 2014 Wiley.

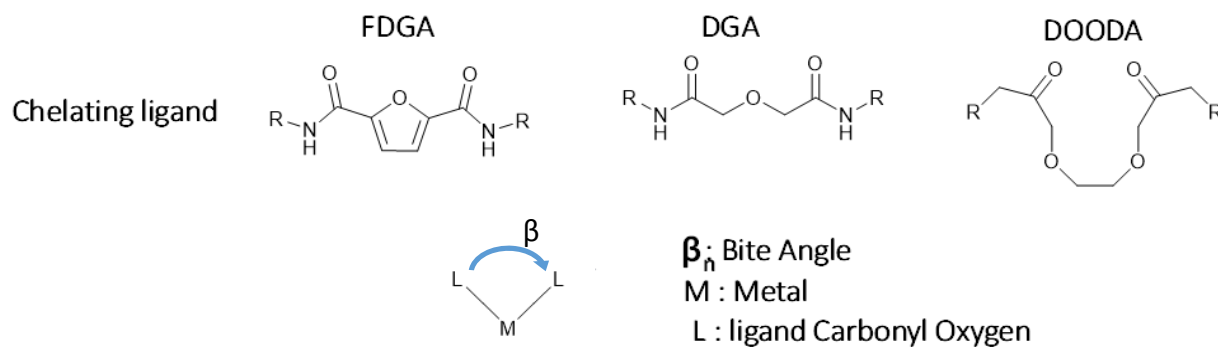


Figure 12 Different bite angles for DGA-analogues. Reproduced with permission from reference [148]. Copyrights 2015 RSC.

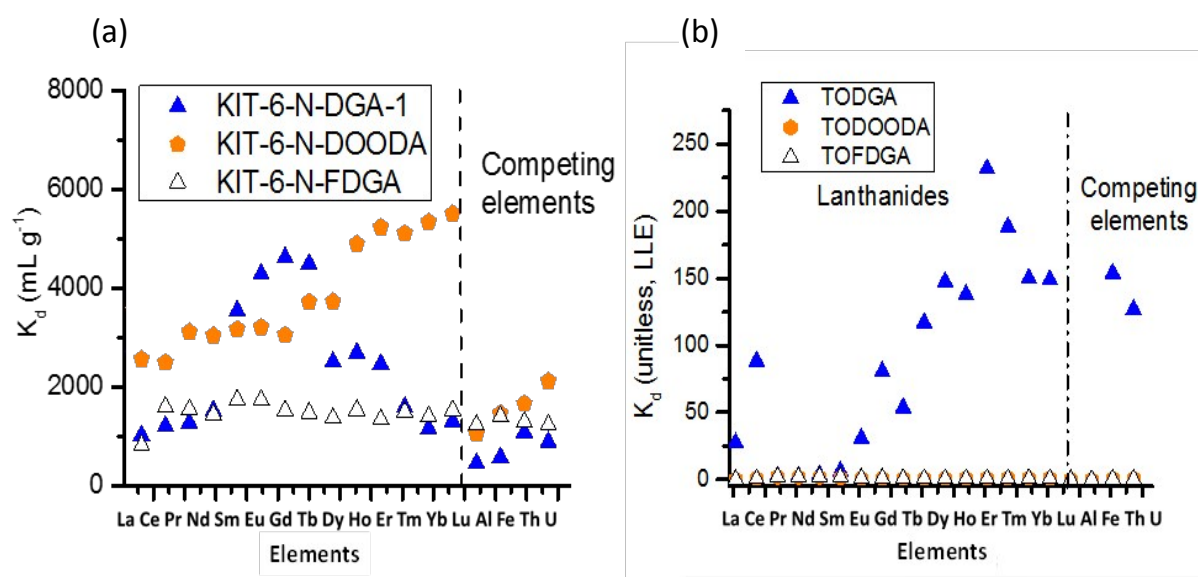


Figure 13 Comparison of the extraction efficiency and selectivity for various DGA-based silica sorbents (a) and ligands in the liquid-liquid phase (b). Reproduced with permission from reference [148]. Copyrights 2015 RSC.



Dr. Justyna Florek studied chemistry at Adam Mickiewicz University in Poznań, Poland. She completed her Ph.D. thesis in 2012 under the supervision of Prof. Maria Ziolk at the Faculty of Chemistry, Department of Heterogeneous Catalysis at Adam Mickiewicz University. In 2012, she joined the group of Prof. Freddy Kleitz at Université Laval, Quebec City (Canada), as a post-doctoral fellow. Her research activity was focused on the synthesis of organo-functionalized nanomaterials exhibiting well-defined pores in the range 1-100 nm with particular emphasis towards environmental and energy applications, in collaboration with the laboratory of Prof. Dominic Larivière (U Laval). Since 2014 she is a professional researcher in Prof. Kleitz laboratory and her current research activity is focused on the synthesis of organo-functionalized nanomaterials for environmental and biomedical applications.



Dr. Simon Giret's educational training is diverse: he earned a BSc in Medicinal Chemistry in 2009 and MSc in Material Chemistry for Health Sciences in 2011 (both from Université Montpellier 2, France), and a PhD Material Chemistry for Health Sciences in 2014, *Hybrid silica nanoparticles as pH-sensitive prodrugs carrier using molecular imprinting* (École Nationale Supérieure de Chimie de Montpellier). Currently, he is a postdoctoral fellow at Université Laval, Quebec City, where his area of research is divided on two axes, first on the development of a process for recovery of rare earth elements using modified mesoporous materials as solid supports and secondly, he is continuing his research on the design of periodic mesoporous organosilicas as drug nanocarriers.

Florek, J. et al.

Biographies



Estelle Juère obtained a DUT (University Diploma of Technology) in Chemistry at IUT Le Mans (France) in 2012 and received her BSc in Plants Chemistry and Natural Products from the University of Quebec at Chicoutimi, UQAC (Canada). In 2013, she started a Master degree in the laboratory of Prof. Freddy Kleitz at Université Laval (Canada) where she is currently a PhD student. Her research focused first on the selective extraction of REEs using ordered mesoporous materials and she is now working on the design of new drug delivery nanoparticles for biomedical applications.



Dominic Larivière is an Associate Professor in the Department of Chemistry, Université Laval. He received his PhD from Trent University (Ontario, Canada) in 2005 under the supervision of Prof. R.D. Evans and R.J. Cornett. Since 2009, he is the director of the Radioecology Laboratory, a university-based research laboratory dedicated to the assessment of radioactivity in the environment and the biota. Dominic and his research group are currently involved in the

Florek, J. et al.

Biographies

development of new radiochemical separations and detection tools, especially for actinides. He is also actively involved in the development of new analytical strategies for the separation and quantification of rare earth elements in both mineral samples and spent fuel.



Freddy Kleitz initially studied chemistry at the Université Louis Pasteur of Strasbourg, France. He received his PhD degree in chemistry in 2002 from the Max-Planck-Institut für Kohlenforschung and the Ruhr University Bochum (Germany) under the supervision of Prof. F. Schüth. He then joined the Korea Advanced Institute of Science and Technology (KAIST, Korea) as a postdoctoral fellow. In February 2005, he joined the Department of Chemistry of Université Laval (Canada). He was awarded the Canada Research Chair on Functional nanostructured materials (Tiers 2). Since 2014, he is a Full Professor in the Department of Chemistry of Université Laval. His main research interests are the design of functional nanoporous materials and exploring their properties as selective sorbents, heterogeneous catalysts and biomedical materials. He has published over 100 refereed research articles. Since October 2014, he is also a guest Professor at the China University of Petroleum in Qingdao, China.

Florek, J. et al.

Graphical abstract